INVESTIGATION OF EFFECTS OF CURRENT AND TEMPERATURE ON EMISSION SPECTRA OF A GALLIUM-NITRIDE-BASED BLUE LASER DIODE

BY

TAOFEEK OLAWALE ADIGUN

A Thesis Presented to the
DEANSHIP OF GRADUATE STUDIES

KING FAHD UNIVERSITY OF PETROLEUM & MINERALS

DHAHRAN, SAUDI ARABIA

In Partial Fulfillment of the
Requirements for the Degree of

MASTER OF SCIENCE

In

PHYSICS

April 2016

KING FAHD UNIVERSITY OF PETROLEUM & MINERALS

DHAHRAN- 31261, SAUDI ARABIA

DEANSHIP OF GRADUATE STUDIES

This thesis, written by TAOFEEK OLAWALE ADIGUN under the direction of his thesis advisor and approved by his thesis committee, has been presented and accepted by the Dean of Graduate Studies, in partial fulfillment of the requirements for the degree of **MASTER OF SCIENCE IN PHYSICS.**

Dr. Watheq Ahmad Al-Basheer
(Advisor)

Dr. Abdullah A. Al-Sunaidi
Department Chairman

Dr. Abdul-Aziz Al-Jalal
(Co-Advisor)

Dr. Salam A. Zummo
Dean of Graduate Studies

Dr. Fida F. Al-Adel
(Member)

24/5/16
Date

Dr. Hocine Bahlouli
(Member)

Dr. Khalil Harrabi
(Member)

I dedicate this work to my parents Mr. Said Adigun and Mrs. Hafdhah Yusuf who have been giving me supports to be successful in life since I came into this world.

ACKNOWLEDGMENTS

All praise and adoration be to Allah for the successful completion of carrying out a study of one of His creation, light.

I would like to show a gratitude to the assistance given to me by my advisor, Dr. Watheq Ahmad Al-Basheer from the start of this study till the end. I have so much benefitted from his pieces of advice since he agreed to be my thesis advisor. There has never been any time lag to my correspondence to him; he attended to any challenge that came up during the experimental part of this work. His effort in making sure that I progress in my academic pursuits is a remarkable one.

Dr. Abdul-Aziz Al-Jalal, my co-advisor, is another man I will continue to remember for the rest of my life for insightful contribution to the success of my work. I appreciate his technical assistance he rendered during the laboratory work of this thesis. My present skills in programming with LabVIEW and Mathematica which I utilized during the laboratory work and data analysis are traceable to him.

I would also like to appreciate the concerted efforts of members of thesis committee, Prof. Fidal Al-Adel, Prof. Hocine Bahlouli and Dr. Khalil Harrabi. I thank them for their constructive critics of my thesis report.

Other people that were responsible for the success of my laboratory work were Mr. Sreedharan Pillai and Mr. Jun (the machinist) at the Energy Lab. Mr. Pillai gave a lot of technical assistance to me in the laboratory and Mr. Jun helped to fabricate some parts in my experimental setup.

I acknowledge the supports given by Physics department and the entire members of staff.

Last but not the least, I would like to show my acknowledgment to the financial support provided by King Abdulaziz City for Science and Technology (KACST) through Science and Technology Unit at King Fahd University of Petroleum and Minerals (KFUPM) for funding this work through the project No. 12-ENV235-04. Also, I would like to acknowledge support provided by the Deanship of Scientific Research at King Fahd University of Petroleum and Minerals (KFUPM) under internal research grants number RG1320-1 and RG1320-2.

TABLE OF CONTENTS

LIST OF TABLES

LIST OF FIGURES

LIST OF ABBREVIATIONS

AlN	:	Aluminum nitride
CCD	:	Charge-coupled device
CW	:	Continuous wave
DBR	:	Distributed Bragg Reflector
DFB	:	Distributed Feedback
DH	:	Double Heterostructure/Heterojunction
FP	:	Fabry-Perot
GaN	:	Gallium nitride
InN	:	Indium nitride
Kr	:	Krypton
L-I	:	Light output - current
LED	:	Light Emitting Diode
lvm	:	LabVIEW measurement
LD	:	Laser Diode
MOS	:	Metal Oxide Semiconductor
PC	:	Personal Computer
RCA	:	Radio Corporation of America
Si	:	Silicon

ABSTRACT

Full Name : Taofeek Olawale Adigun

Thesis Title : Investigation of Effects of Current and Temperature on Emission Spectra of a Gallium-nitride-based Blue Laser Diode

Major Field : Physics

Date of Degree : May 2016

Most of the applications where gallium nitride (GaN)-based blue laser diodes are utilized require high laser spectral quality with controlled spectral wavelength and stable output power. Owing to these requirements, it is important to characterize commercial blue laser diodes prior to employing them in spectroscopy and other applications. In this study, highly resolved emission spectra of a Roithner LaserTechnik LD-445-50PD Fabry-Perot GaN blue laser diode, over the wavelength region (440 – 450 nm), will be measured and analyzed to study the evolution and stability of the longitudinal modes of a single-transverse mode laser diode. The emission spectra of the laser diode will be experimentally investigated as a function of operating current and temperature and over continuous operation time. Moreover, laser diode's temporal stability will be investigated by monitoring emitted spectra intensity variation while selecting and monitoring a single longitudinal mode, at fixed current and temperature and over extended period of lasing. The proposed technique will be utilized to evaluate few optical parameters related to the properties of GaN-based blue laser diodes, such as mode spacing, optical gain, threshold current, slope efficiency (or external differential) and wavelength rate of change with temperature and injection current. The main purpose of this study is to map the evolution of the longitudinal modes of a commercial GaN-based blue laser diode. The successful

application of the proposed research herein is anticipated to provide scholars and users much needed information on the operation and nature of emission spectra of GaN-based blue laser diodes.

ملخص الرسالة

الاسم الكامل: توفيق اولال أديغن

عنوان الرسالة: التحقيق في آثار التيار الكهربائي ودرجة الحرارة على الانبعاثات الأطياف من الصمام الثنائي ليزر أزرق مصنوعة من نيتريد الغاليوم

التخصص: الفيزياء

تاريخ الدرجة العلمية: مايو 2016

معظم التطبيقات التي نيتريد الغاليوم (الجاليوم) القائم على الثنائيات الليزر الزرقاء تستخدم تتطلب أشعة الليزر عالية الجودة الطيفية مع الطول الموجي الطيفي للرقابة وانتاج الطاقة مستقرة. ونظرا لهذه المتطلبات، من المهم أن تميز الثنائيات الليزر الأزرق التجارية قبل توظيفها في التحليل الطيفي وغيرها من التطبيقات .سيتم قياس حلها غاية الانبعاثات الطيفية من الانضباطي فابري بيرو غان الثنائيات الليزر الأزرق وتحليلها لدراسة تطور واستقرار وسائط طولية من الصمام الثنائي ليزر أحادية وضع عرضية. أطياف من اللون الأزرق الانبعاثات استنادا غان (440-480 نانومتر) سيتم التحقيق تجريبيا الثنائيات الليزر بوصفها وظيفة من التشغيل الحالية، ودرجة الحرارة الداخلية ووقت تشغيل المستمر. وعلاوة على ذلك، سيتم التحقيق الثنائيات الليزر درس الاستقرار الزماني من خلال رصد كثافة أطياف المنبعثة الاختلاف مع مراقبة الوضع الطولي المهيمن، وأكثر من 10 ساعة متواصلة من الليزر. وسوف تستخدم هذه التقنية المقترحة لتقييم بعض المعلمات الطيفية ذات الصلة خصائص استنادا غان الثنائيات الليزر الأزرق، أي تباعد وضع وتحقيق مكاسب البصرية. الغرض الرئيسي من البحث المقترح هو رسم خريطة لتطور وسائط طولية من مقرها غان الثنائيات الليزر الأزرق. ومن المتوقع أن تكون لها تطبيقات مباشرة في العديد من المجالات حيث استخدام الثنائيات الليزر هو العمود الفقري لنجاح تنفيذ الدراسة المقترحة. التطبيق الناجح لبحث المقترح هنا ومن المتوقع أن توفر العلماء ومستخدمي المعلومات المطلوبة عن العملية وطبيعة أطياف انبعاث الثنائيات الليزر الأزرق أساس الجاليوم.

CHAPTER 1

INTRODUCTION

Gallium-nitride (GaN) based laser diodes that emit light in the blue region of the electromagnetic spectrum are a group of laser diodes that has attracted the attention of researchers since their development by Nakamura *et al.* [1] and their application has increased tremendously. Due to their emission spectra wavelength, blue laser diodes have many applications in day-to-day activities. Furthermore, their compactness and portability make the integration of gallium-nitride based blue laser diodes with electronic circuits possible. Among the visible light, blue light has the least attenuation after violet light in underwater communications. This makes GaN-based blue laser diode find application in deep water communications [2]. Aside from underwater communications, they find application in high-speed optical communications [3]. In military weaponry, they are also being used as a rangefinder and target designator to reduce collateral damage [4], [5]. Blue laser diodes also serve as pumping source in solid-state lasers [6]. Due to its short wavelength, blue laser can detect smaller size pit in discs unlike the red or infrared laser, as depicted in Figure 1.1. It implies that the shorter the wavelength, the more data the discs can hold. The invention of GaN-based blue laser diode has made it possible to manufacture high density optical storage devices known as Blu-ray discs (BD) [7]. Some infected human body tissues absorb in the blue region of electromagnetic spectrum, thus blue laser diodes also find application in medicine to carry out diagnosis of tissues for infection and bloodless treatments of the tissues [8], [9]. A typical diagnosis application of blue laser diode is shown in Figure 1.2. Blue diodes can also be combined with other primary colors

(red and green) to provide white lightning [10]. Spectroscopic applications that involve emission and absorption in the blue region of electromagnetic spectrum has also utilized GaN-based blue laser diodes to carry out research in environmental monitoring of toxic gases such as oxides of nitrogen (NOx) [11], [12], [13]. There is also an ongoing debate about whether GaN-based blue diodes, with the two other primary colors from other devices, are capable of supplying the light required by plants for their growth, perhaps being a substitute for the genetically grown plants.

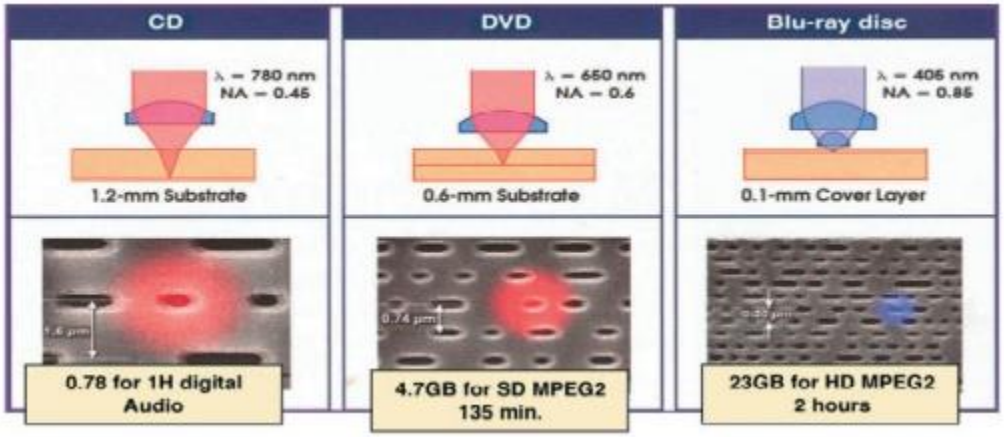

Figure 1.1: Comparison of optical storage formats in discs [7]

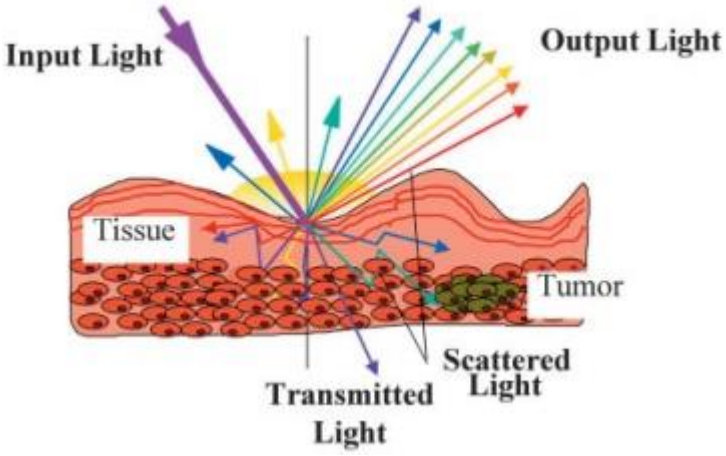

Figure 1.2: An infected tissue undergoing diagnosis by incident with blue laser [7]

1.1 GaN Semiconductor as a Blue Laser

Table 1.1 shows some of the commonly used semiconductors with their band gaps. GaN belongs to subgroup III-nitride of the main group of III-V compound semiconductor. The figure of merit which makes GaN semiconductor promising candidate as an emitter of blue light is the band gap, 3.39 eV [14], [15]. This was known shortly after gallium-arsenide based laser diode emitting in the infrared region of electromagnetic spectrum was demonstrated [16]. Despite this discovery, GaN based laser diode technology did not enjoy rapid development like GaAs. The main obstacle to GaN based laser diode technology was how to develop a conducting *p*-type GaN semiconductor needed to combine with the easily fabricated "undoped" *n*-type GaN semiconductor to form a *p-n* junction. The undoped *n*-type GaN material typically has electron concentration above $10^{19}/\mathrm{cm}^3$ [14]. A research group at RCA (Radio Corporation of America) laboratories in the 1970s made many attempts to fabricate the needed *p*-type GaN but they were unsuccessful and the study was later abandoned [17]–[22]. Worth mentioning is the competition for blue light between GaN and zinc-selenide (ZnSe), which belongs to the II-IV semiconductor group. ZnSe is a wide band gap [23] semiconductor like GaN, so this makes it a rival candidate for blue light emitting device as demonstrated by Okuyama *et al.* [24] and Boney *et al.* [25].

However, the first successful fabrication of the formerly elusive conducting *p*-type GaN by Amano *et. al* [26] and then followed by Nakamura et. al [27] shifted attention away from the ZnSe material due to its relatively short lifetime [28]. This breakthrough led to the first GaN based blue laser diode operating under pulsed injection current [1] and continuous-wave [29] at room temperature in 1995 and 1997, respectively. In 1999, Shuji

Table 1.1: Physical properties of some semiconductors. E_g is the band gap, $\mathrm{d}E_g/\mathrm{d}T$ temperature dependence of the band gap, λ_g is the wavelength corresponding to the band gap, $n(\lambda_g)$ is the dispersive refractive index and $\mathrm{d}n/\mathrm{d}T$ is the temperature dependence of the refractive index [30]

Semiconductor	E_g(eV)	Type	$\mathrm{d}E_g/\mathrm{d}T$ (meV/K)	λ_g (μm)	$n(\lambda_g)$	$\mathrm{d}n/\mathrm{d}T$ ($10^{-5}\mathrm{K}^{-1}$)
Group IV						
Ge	0.66	I	−0.37	1.87	4	27.6
Si	1.12	I	−0.25	1.11	3.45	13.8
III-V Compounds						
GaAs	1.42	D	−0.45	0.87	3.6	15
GaN	3.39[a]	D	−0.45	0.36	2.6	6.8
II-VI Compound						
ZnSe	2.67[b]	D	−0.50	0.46	2.3	6.3

[a]see ref. [14]; [b]see Ref. [23]

Nakamura, former Nichia Chemical Industries employer, released GaN based blue/violet laser diodes in the market [31]. Since its development, GaN based laser diode technology has significantly improved, consequently and many areas of applications have emerged [32]. It is clearly shown from Table 1.1 that GaN semiconductor can inherently emit light in the violet region of electromagnetic spectrum. So in order to extend the emission into the blue region, GaN can be alloyed with other semiconducting materials. This is achieved

by alloying GaN with other members of III-nitride semiconductor which include indium and aluminum nitrides (InN, AlN) to form either ternary or quaternary (or more) GaN-based compound semiconductors. The resulting band gaps or wavelengths would depend on the stoichiometry composition of the individual materials. The band gaps of InN and AlN are 0.6 and 6.2 eV, respectively, consequently GaN band gap can be engineered by the utilizing InN and/or AlN to obtain the desired band gaps or wavelengths [33], [34].

1.2 Statement of Research Problem

Fabry-Perot laser diodes are the most common and cheapest laser diodes. Multiple resonant modes which have oscillation with several longitudinal modes are a characteristic of Fabry-Perot laser diodes. The output parameters such as optical power and emission spectrum of a Fabry-Perot laser diode are sensitive to change in injection current and operating temperature. The output optical power of laser diode at some fixed injection current and temperature does not remain the same whenever one of the operating conditions changes. Likewise, the spectral emission of the laser diode responds to change in the operating parameters. There are shifts in the longitudinal modes and gain profile of the laser diode as injection current and/or temperature change. Thus, both laser diode injection current and temperature are used to tune or shift the wavelength to the specific wavelengths required. Wavelength tuning is an important tool for selecting the desired wavelengths for different applications such as spectroscopy where the wavelengths are scanned over some range. For a particular application, a certain fixed injection current at a fixed laser diode temperature might give a desired result but once there is a change of ambient temperature of the laser diode to higher temperature, the injection current might not be safe any longer for application at the new temperature [35]. Application areas of blue laser diode such as

medicine, spectroscopy and optical/underwater communications require high spectral purity and stability. So an injection current-temperature combination, that would give high spectral purity and stability, is the ultimate goal in spectroscopic research. Thus, a great deal of attention is needed by spectroscopic researchers in selecting optimum injection current and temperature that is suitable for their studies. Though GaN semiconductors are relatively stable to temperature change and even perform well at elevated temperature as compared with GaAs, Fabry-Perot GaN-based blue laser diodes exhibit these injection current and temperature characteristics on their output emission.

1.3 Statement of research aim and objectives

The ultimate goal in spectroscopic application of a GaN based blue laser diode is to have high spectral emission stability with high resolution for the purpose of carrying out studies on detection and monitoring of toxic gases, such as oxides of nitrogen and sulphur. In order to achieve this, it is imperative to characterize the laser diode for some optimal injection current and temperature for its subsequent spectroscopic application.

In this thesis, highly resolved spectral emission of a Roithner LaserTechnik LD-445-50PD tunable Fabry-Perot GaN blue laser diode, emitting radiation over the wavelength region 440 – 450 nm, will be measured and analyzed to study the evolution and stability of the longitudinal modes of a single-transverse mode laser diode. The emission spectra of the laser diode will be experimentally investigated as a function of operating current and temperature and over continuous operation time. This study will be carried out based on the following objectives:

1. To investigate the temporal stability of the laser diode output optical power and wavelength at some fixed injection current and temperature over an extended period of time.
2. To estimate the laser diode lasing parameters such as threshold current, characteristic temperature from light output-current (*L-I*) curve and differential quantum efficiency-temperature curve.
3. To investigate the evolution of longitudinal modes peaks location as a function of injection current as well as temperature
4. To evaluate current and temperature coefficients of the laser diode emission wavelength and mode spacing.

1.4 Structure of the Thesis

The outline of the chapters in this thesis is as follows: chapter 2 discusses the theoretical background of basic double heterojunction Fabry-Perot (FP) laser diodes. Definitions of some laser diode output parameters and their relationship with change in injection current and operating temperature are also explained. Chapter 3 gives the experimental details of the present study while Chapter 4 presents the results and discussion of the experimental observation. Finally, conclusion and summary of the study are given in Chapter 5.

CHAPTER 2

THEORETICAL BACKGROUND OF LASER DIODES

This chapter gives a brief physical basis of a double heterojunction laser diode and goes on to present the principle of operation of a Fabry-Perot laser diode. Theoretical background of a Fabry-Perot laser diode based on recombination mechanism in the active layers. The laser diode emission characteristics are also discussed in addition to their relationships with injection current and operating temperature.

2.1 Basic Structure of a Double Heterojunction Laser Diode

Every laser must have three basic components, namely, an active or gain medium, a pumping source and an optical feedback mechanism. The first set of laser diodes that were fabricated were homojunction *p*-*n* semiconductor structures. A homojunction laser diode is the kind of laser diode structure in which the *p*- and *n*-type are made from similar material such as *p*-GaN/*n*-GaN and the junction serves as the active medium. Homojunction laser diodes suffer from two major problems and for these reasons, it has become obsolete. A homojunction laser diode has a very high threshold current which makes it not suitable for continuous wave (cw) operation at room temperature [36], [37]. Also, a large percentage of the photons generated from electron-hole recombination are absorbed by the *p*- and *n*-type semiconductors, thus reducing the efficiency of the laser diode [4]. Another kind of laser diode structure is the double heterojunction (DH) structure. Nowadays, commercially available laser diodes are basically made of DH structure. A DH structure is formed by two

dissimilar semiconductor materials of different band gaps such as (Al, In)GaN/GaN. The active layer, with band gap $E_{g,a}$, is, basically an undoped semiconductor sandwiched between two distinctly doped semiconductor cladding layers of wider band gap $E_{g,cl}$ (i.e. $E_{g,cl} > E_{g,a}$). Thus the active layer has larger refractive index. Figure 2.1 shows a schematic view of a laser diode made from a *p*-type and *n*-type AlGaN as cladding layers and an undoped InGaN active layer.

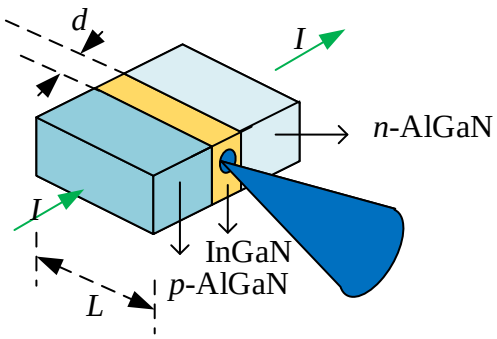

Figure 2.1: Schematic diagram of the generic chip of a laser diode. *I* is the injection current to drive the laser diode. *L* is the physical length of the active layer of the laser diode. The cone is used to depict the laser emission.

2.2 Principle of Operation of Laser Diodes

When a DH laser diode is formed, the Fermi energy levels align themselves as shown in Figure 2.2. However, when it is forward biased by a voltage V_F, the Fermi level splits into two quasi-Fermi levels E_{FC} and E_{FV} with separation eV_F in the active layer as depicted in Figure 2.3. Electrons from the *n*-type and holes from the *p*-type semiconductor cladding layers are injected into the active layer and are confined within the potentials created by the active layer [38], [39]. Radiative and/or nonradiative recombination of the electrons and the holes occurs where the radiative recombination leads to emission of photons while

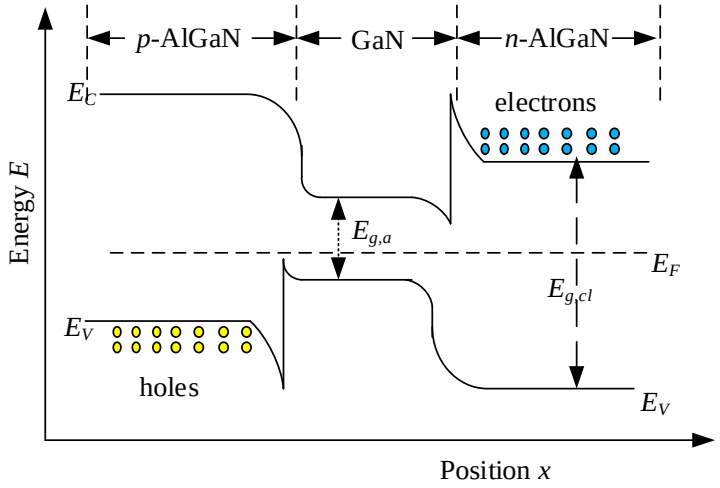

Figure 2:2: Energy band diagram of a DH structure of a p-i-n laser diode. Under zero-applied forward bias voltage, the Fermi levels V_F of the layers are aligned. E_C and E_V are the conduction and valence band energy respectively, while , $E_{g,a}$ and $E_{g,cl}$ are the bandgap energies of the active and cladding layers, respectively.

the nonradiative recombination produces no photon emission. The energy, $E = hv$, carries by each of the emitted photons corresponds to the energy bandgap of the active layer.

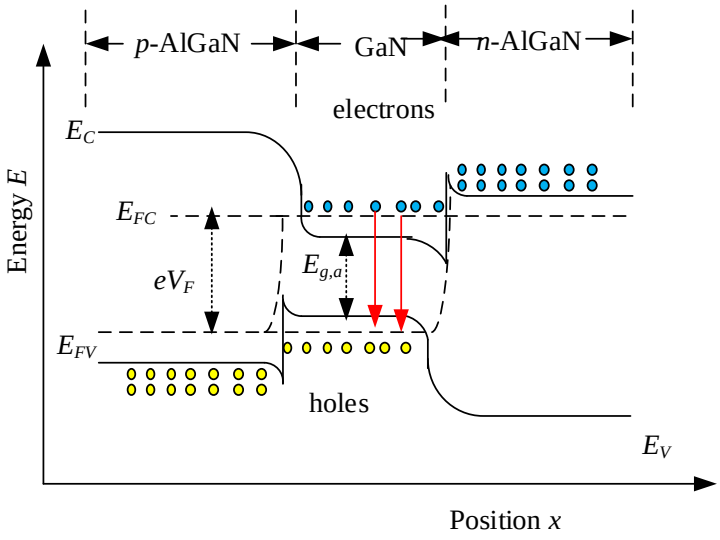

Figure 2.3: Energy band diagram. The Fermi levels separates into two quasi-Fermi levels, , E_{FC} and E_{FV} upon application of forward bias with energy spacing eV_F, where e and V_F are electronic charge and forward bias voltage respectively

The emitted photons are distributed in random directions and are out of phase from one another. This is known as spontaneous emission and is obtainable in light emitting diodes

as shown in Figure 2.4(a). In order for lasing action to take place, an optical feedback mechanism which is provided by cleaving the two end facets of the semiconductor crystal to form resonant cavity. This type of resonant cavity is known as Fabry-Perot cavity and is discussed in section 2.3.2.2.

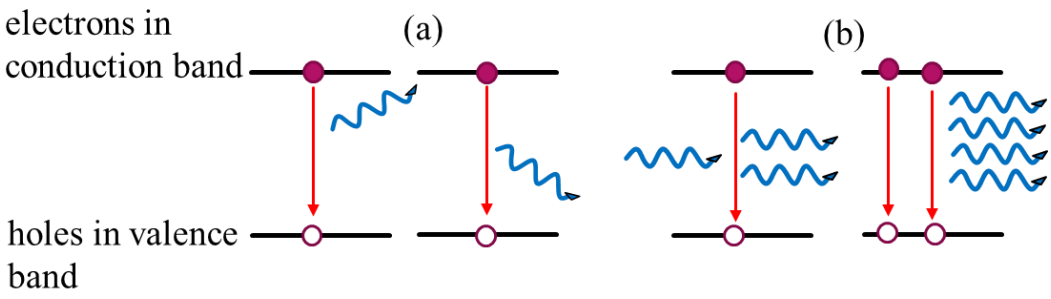

Figure 2.4: Recombination of electrons and holes generate photons (a) spontaneous emission dominates. The photons emitted are in random direction. (b) stimulated emission dominates. The photons emitted are in phase and same direction

As more and more photons are generated from the recombination of electrons and holes, the photons undergo multiple reflections as they travel back and forth from one end facet to another. They also stimulate the injected electrons in the active layer to recombine with holes to emit other photons which are in the same direction and phase with the stimulating photons as shown in Figure 2.4(b). When stimulated photon emission is dominant over the spontaneous emission and the absorption by the cladding layers, optical gain and coherent emission is achieved. The minimum current required for stimulated emission to equal spontaneous emission and absorption in a laser diode is known as the laser diode threshold current.

Since the bandgap of the active layer is less than that of the cladding layers, thus the active layer refractive index is greater than that of the cladding layers, and consequently, the photons are confined in the active layer due to total internal reflection at the interface of the active and cladding layers. Furthermore, reflectivity at each of the two end facets of the

Fabry-Perot cavity is obtained as result of discontinuity in index of refraction of the laser diode active layer and air. For a typical refractive index of a GaN-based blue laser diode, the refractive index is $n = 2.9$ [40], therefore its reflectivity is

$$R = \frac{(n-1)^2}{(n+1)^2} = 0.24$$

However, the reflectivity can be enhanced by coating the reflective surfaces of the two cleaved end facets with dielectric thin film [41].

In practice, most of laser diodes have more than three layers in order to obtain better optical characteristics [40], [41].

2.3 Output Characteristics of a Laser Diode

2.3.1 Laser Diode Output Optical Power

A laser diode begins lasing only at an injection current above its threshold current below which spontaneous emission is dominant, which is a characteristic of light emitting diodes (LEDs). The output optical power of the laser diode increases rapidly at injection current well above the threshold current. A typical laser diode plot of output optical power versus injection current is shown in Figure 2.5. The curve is commonly referred to as *L-I* curve, that is, the light output-injection current curve.

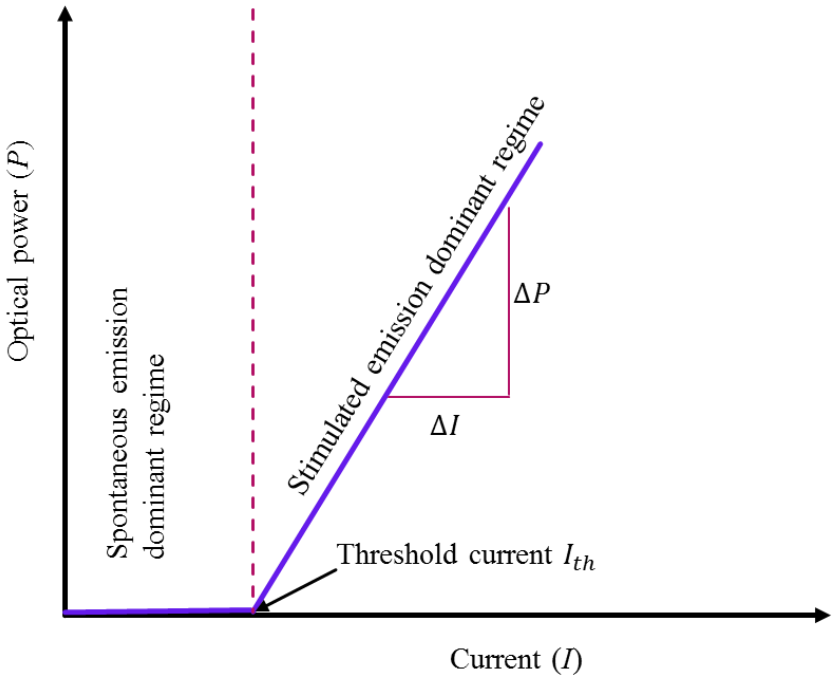

Figure 2.5: Laser diode *L-I* curve. Spontaneous emission of photons is dominant at injection current below the threshold current I_{th}. Stimulated emission of photons dominates above the threshold current.

The slope of the laser diode *L-I* curve can be obtained at an injection current above the threshold current and it is known as the slope efficiency S_{L-I} of the laser diode. It provides information about how the injection current produces output optical power and expressed as

$$S_{L-I} = \frac{\Delta P}{\Delta I} \tag{2.1}$$

with unit of milliwatt per milliampere (mW/mA). The threshold current I_{th} of the LD can approximately be determined by extrapolation from the linear fit of the *L-I* curve where the line intersects injection current (*I*) axis at zero output optical power (*P*).

Other laser diode parameter that can be estimated from *L-I* curve includes external differential quantum efficiency, η_{ext} (a unit-less parameter) [42].

External differential quantum efficiency is the ratio of number of photons that is emitted to the number of electron-hole pair recombination. In a perfect laser diode, it is 1 (that is 100 percent) because each of the recombination events produces one photon that contributes to the laser diode light output. However in real laser diode, not all photons generated from the electron-hole pair recombination are contribute to a laser diode output. Some photons are lost due to their absorption by the internal structure of the semiconductors.

In order to derive an expression for a laser diode external differential quantum efficiency, a comparison between the slope efficiency of a real laser diode is made against that of an ideal one. Consider a current *I* (electronic charge per unit time, e/t) injected into a perfect laser diode which gives an output power *P* (photon energy per unit time, E/t), where *E* is expressed as

$$E = \frac{h\,c}{\lambda} \tag{2.2}$$

in Joule. The slope efficiency of a perfect laser diode can therefore be expressed as

$$S_{L-I*} = \frac{h\,c}{\lambda\,e} \tag{2.3}$$

where c and λ are the photon's speed and wavelength respectively, and h is the Planck's constant. The ratio of the slope efficiency of a real laser diode to that of the perfect one can now be written as

$$\frac{S_{L-I}}{S_{L-I*}} = \frac{\Delta P}{\Delta I} \Big/ \left(\frac{h\,c}{\lambda\,e}\right) \tag{2.4}$$

from which the external differential quantum efficiency per facet η_{ext} of a real LD can be obtained as

$$\eta_{ext} = \lambda \, S_{L-I} \left(\frac{e}{h \, c}\right) \tag{2.5}$$

External differential quantum efficiency is a dimensionless parameter. For most laser diodes, the external differential quantum efficiency is over the range 0.25 and 0.60 [43], [44].

2.3.2 Laser Diode Spectral Emission Characteristics

2.3.2.1 Effect of Injection Current on Spectral Properties of a Laser diode

Injection current into a laser diode causes electrons and holes from *n*-type and *p*-type laser diode cladding layers, respectively, to be injected into the active layer of the laser diode where they recombine to emit photons. Radiative recombination of the carriers leads to build up of optical gain in the active layer as shown in Figure 2.6.

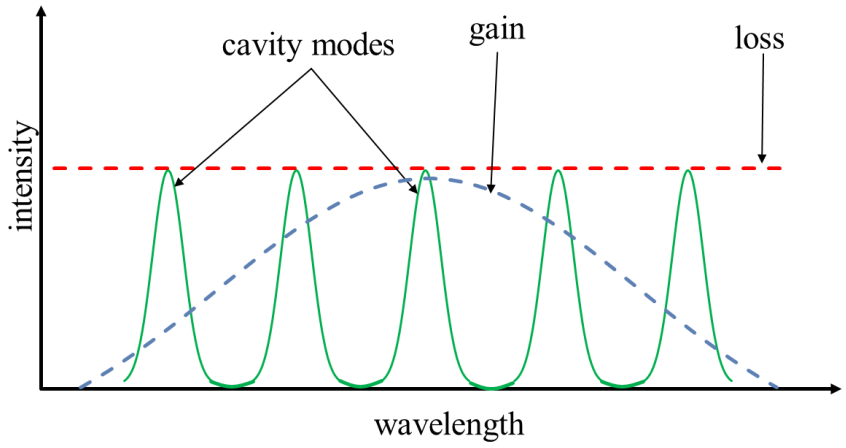

Figure 2.6: Optical gain of laser diode below threshold current. The gain is less than the loss.

The emitted photons undergo several reflections between the two cleaved end facets of the FP cavity as they travel through the laser diode active layer. The spectrum labeled "gain" in Figure 2.6 is a typical gain profile for an injection current below the threshold. Here, the optical gain is less than sum of all the losses, and thus the spontaneous emission of photons is more dominates. The losses can result from but not limited to premature or undesired transmission of photons due to mirror reflectivity below 100%, emitted photons that do not propagate in directions that satisfy total internal reflection get absorbed by the cladding layers and some absorbed by the active layer. Another form of loss may be due to inhomogeneity of the active layer structure which results in scattering of photons [45]. However, only the photons that survive these losses are fed back into the active layer where they are amplified by stimulating recombination of the injected electrons and holes.

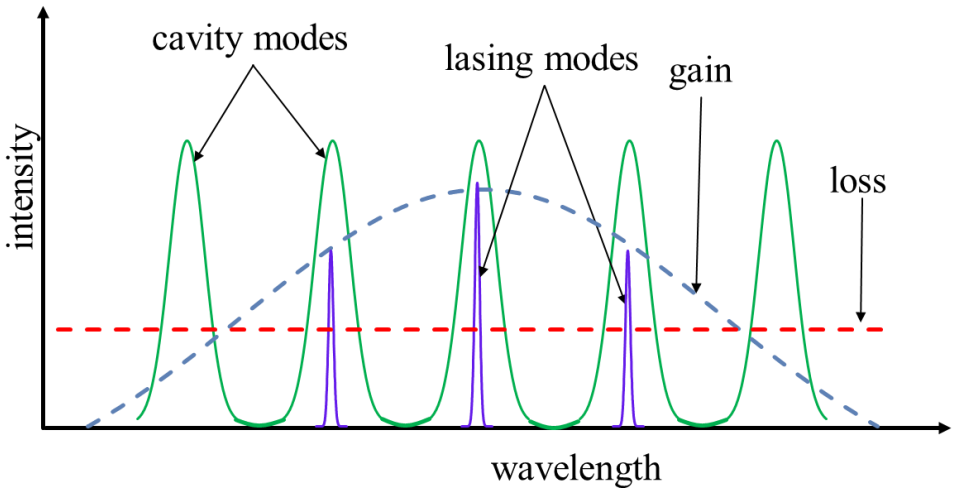

Figure 2.7: Optical gain of laser diode at threshold current. The gain is equal to the loss and thus the laser diode lases

The gain can be enhanced by increasing the injection current, thus increasing the concentration of electrons and holes at the active layer where the recombine to yield more photons. When the threshold current of the laser diode is reached, the optical gain equals

to the sum of all the losses and consequently, stimulated emission of photons becomes dominant over that of spontaneous. At the threshold current, an FP laser diode exhibits several longitudinal modes which are evenly spaced as shown in Figure 2.7. The modes shift to higher wavelengths with increase in injection current above the threshold, so the current coefficient of this shift in wavelengths of the modes can be experimentally evaluated [46]–[48].

2.3.2.2 Longitudinal Modes

The resonant cavity in an FP laser diode provides the optical feedback mechanism for the photons in the active laser. Figure 2.8 shows a Fabry-Perot resonator which is formed by two parallel mirrors placed at a distance *L* apart. When light travels back and forth between the two mirrors, only those wavelengths which satisfy the standing wave relation

$$nL = m\frac{\lambda}{2} \tag{2.6}$$

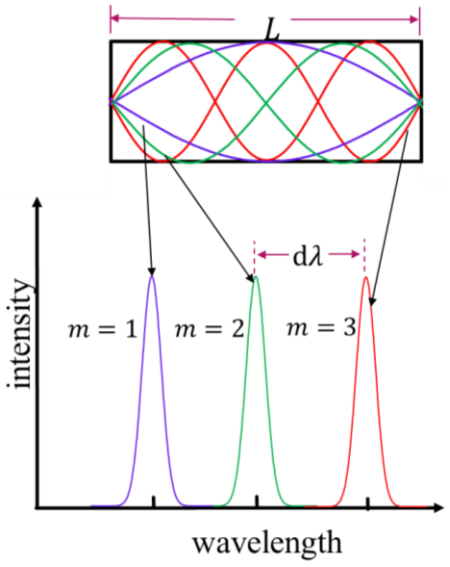

Figure 2.8: Schematic view of standing wave in a Fabry-Perot cavity with three standing waves (top) which correspond to the three longitudinal modes for m=1, m=2 and m=3 (bottom)

are allowed to resonate in the cavity. Where L is the cavity length, λ is the photon wavelength, m is an integer and n is the effective or group refractive index of the resonator. In laser diode, the resonator is formed by the active layer and its two cleaved end facets. The photons generated by carrier recombination in the active layer of the laser diode undergo multiple reflections between the two cleaved end facets of the cavity.

The order m that is expected in this study can be obtained analytically by using a typical value of a GaN laser diode active layer cavity length of 650 μm which has group refractive index of 2.9, for wavelength $\lambda = 448$ nm as

$$m \approx \frac{2 \times 2.9 \times 650 \times 10^{-6}}{448 \times 10^{-9}}$$

$$\approx 8415$$

Laser diode optical power is distributed among the lasing modes where the mode with highest intensity takes the highest optical power [49]. The longitudinal modes constitute the laser spectrum and the mode with the highest intensity is closer to the lasing gain spectrum [50].

2.3.2.3 Mode spacing

The wavelength difference $\mathrm{d}\lambda$, between two adjacent modes is known as mode spacing of the longitudinal modes in a Fabry-Perot cavity. The mode spacing can be obtained by taking the derivative $\mathrm{d}m/\mathrm{d}\lambda$, from equation (2.6)

$$\frac{\mathrm{d}m}{\mathrm{d}\lambda} = 2L\left(\frac{1}{\lambda}\frac{\mathrm{d}n}{\mathrm{d}\lambda} - \frac{n}{\lambda^2}\right) \tag{2.7}$$

where $\mathrm{d}n/\mathrm{d}\lambda$ implies a dispersive material semiconductor, that is, the effective refractive index changes with photon wavelength. Setting $\mathrm{d}m = -1$,

$$\frac{-1}{\mathrm{d}\lambda} = 2L\left(\frac{1}{\lambda}\frac{\mathrm{d}n}{\mathrm{d}\lambda} - \frac{n}{\lambda^2}\right) \tag{2.8}$$

From which

$$\mathrm{d}\lambda = \frac{\lambda^2}{2L\left(n - \lambda\frac{\mathrm{d}n}{\mathrm{d}\lambda}\right)} \tag{2.9}$$

or

$$\mathrm{d}\lambda = \frac{\lambda^2}{2Ln_{eff}} \tag{2.7}$$

where $n_{eff} = n - \lambda\frac{\mathrm{d}n}{\mathrm{d}\lambda}$ is the group refractive index [41].

When the mode spacing of a laser diode spectrum is known, it is possible to estimate the length of the laser diode active layer, that is, cavity length [43] from equation (2.10). By using typical value of a GaN laser diode active layer cavity length of 650 μm which has group refractive index of 2.9 [40], the longitudinal mode spacing, $\mathrm{d}\lambda$ can be obtained for wavelength $\lambda = 448$ nm as

$$\mathrm{d}\lambda = \frac{(448 \times 10^{-9})^2}{2 \times 2.9 \times 650 \times 10^{-6}}$$

$$= 0.0532 \text{ nm}$$

This mode spacing is compared with the one that is experimentally obtained in this study.

2.3.3 Temperature effects on *L-I* Curve and its Derivative Parameters

Change in temperature of laser diode affects the carrier concentrations at the active layer of laser diode. When the operating temperature is increased, the laser diode gain decreases, therefore the threshold current shifts to higher value. Consequently, the laser diode *L-I* curve responds to the temperature change accordingly as shown in Figure 2.9. So in order to maintain a certain optical power when there is an increase in temperature, more injection current. Not only that the threshold current shifts to a higher value as laser diode temperature increases but also the slope efficiency of the laser diode decreases as depicted in Figure 2.9. These undesirable increase of threshold current and decrease in slope efficiency are due to the loss of carriers (electrons and holes) which results from flow of injection current around the active layer which very severe at high temperature.

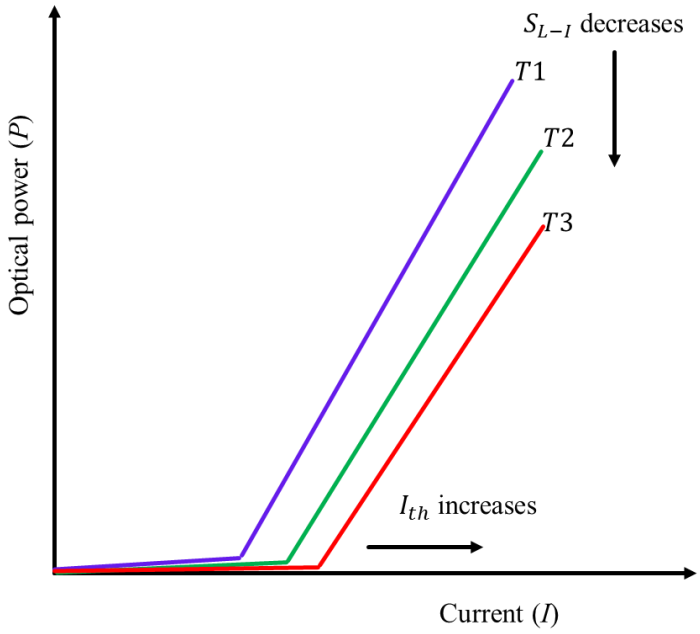

Figure 2.9: Temperature dependence of laser diode threshold current and slope efficiency (external differential quantum efficiency), where $T_3 > T_2 > T_1$

The dependence of a laser diode threshold current on operating temperature is given by the empirical relation

$$I_{th}(T) = I_{th0}\exp(T/T_0) \tag{2.8}$$

I_{th} is the threshold current at a temperature T, I_{th0} is the initial threshold current at $T = 0$ and T_0 is the characteristic temperature of the LD [51]. T_0 can be determined by taking the first derivative of equation 2.8 with respect to T,

$$\ln I_{th}(T) - \ln I_{th0} = T/T_0 \tag{2.9}$$

which yields

$$\mathrm{d}[\ln I_{th}(T)] = \mathrm{d}T/T_0 \tag{2.10}$$

or

$$T_0 = \frac{\mathrm{d}T}{\mathrm{d}[\ln I_{th}(T)]} \tag{2.11}$$

T_0 is therefore the inverse of the slope the threshold current versus temperature curve

$$T_0 = \frac{\Delta T}{\Delta \ln I_{th}} \tag{2.12}$$

A higher characteristic temperature indicates a lower sensitivity of a laser diode threshold current when there is a relatively large change in temperature, and vice versa [43], thus a high T_0 indicates a thermally stable laser diode. Generally, GaN semiconductor laser diodes have relative high T_0 [52].

2.3.4 Effect of Temperature on Spectral Properties of a Laser diode

Effect of change in temperature of a laser diode includes change in physical length *L* of the laser diode active layer due to thermal expansion, change in the refractive index of the active layer as result of the carrier concentration distribution and change in size of the active layer band gap. Since the wavelength of a longitudinal mode is proportional to the physical length *L* (equation 2.6) of the active layer which forms the resonator cavity, a change in *L* as a result of thermal expansion when a laser diode operating temperature is increased would shift the longitudinal mode to a higher wavelength as shown in Figure 2.10.

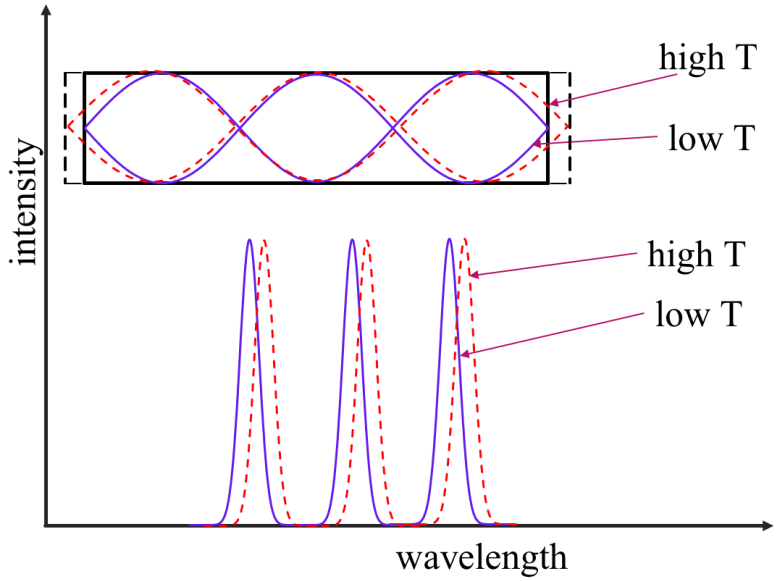

Figure 2.10: Thermal expansion of the resonator cavity (top) and the corresponding longitudinal mode shift with temperature (bottom). "high T" and "low T" denote high and low temperature respectively.

Similarly, the refractive index *n*, depends on carrier concentration at the active layer. So even if there is no expansion of the active layer, the effective optical length (*nL*) traveled by photons changes due to the change in the refractive index. Therefore, there is a shift in

the longitudinal mode wavelength according to equation (2.6). However, the carrier concentration at the active layer is pinned at the laser diode threshold current, therefore, the contribution of carrier concentration to change in the refractive index stops [41]. More injection current into the active layer leads to Joule heating which would later results in change in the refractive as well as the thermal expansion of the active layer, as explained above. The change in refractive index as a result of temperature change is expressed as [41]

$$\Delta n = (2\sim5) \times 10^{-4} \Delta T \tag{2.13}$$

Temperature coefficients $\Delta n/\Delta T$ of GaN-based semiconductors have been experimentally and theoretically studied [53]–[55]. The shifts in longitudinal mode wavelengths of the laser diode due to changes in physical and optical length of resonator cavity of the laser cause the changes in the laser diode gain profile.

The third effect, reduction in band gap size as a result of increase in temperature mainly affects the gain curve peak wavelength and shifts to higher wavelength [39], as illustrated in Figure 2.11.

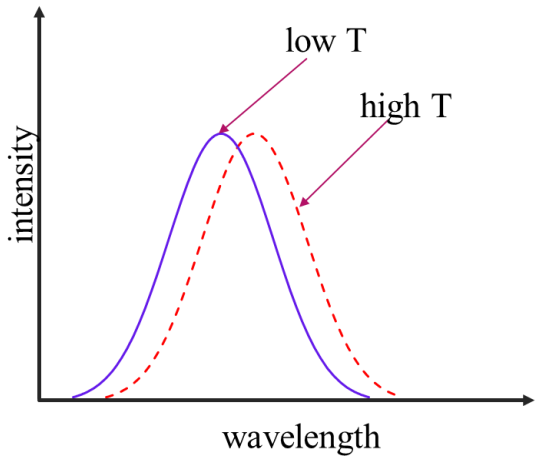

Figure 2.11: Shift of gain peak to higher wavelength as a result of decrease in bandgap when temperature is increased

The temperature coefficients of the longitudinal mode wavelength $\mathrm{d}\lambda_m/\mathrm{d}T$ and the gain peak wavelength $\mathrm{d}\lambda_g/\mathrm{d}T$ can be experimentally evaluated. However, it has been experimentally observed that the shift in wavelength of the gain is a about factor of 3 greater than that of the longitudinal mode wavelengths [46], [56].

CHAPTER 3

EXPERIMENTAL DETAILS

This chapter gives the experimental details and experimental procedures of the study. Figure 3.1 shows the main experimental setup used to investigate the effects of changing current and operating temperature of a GaN-based blue laser diode on its emission spectra. It consists of a GaN blue laser diode which is controlled by current and temperature controller. A high resolution spectrometer which consists of a monochromator coupled with a CCD camera was used to analyze the laser diode spectrum. National Instruments data acquisition devices were used to interface the PC to the laser diode current and temperature controllers for the purpose of data acquisition. Brief details of the workings of the aforementioned components in the setup are presented in the next section. This chapter will be divided into three main sections and presented in the following order: section 3.1 gives the details of the laser diode employed; section 3.2 discusses the principle of operation of the spectrometer and its calibration; and the data acquisitions.

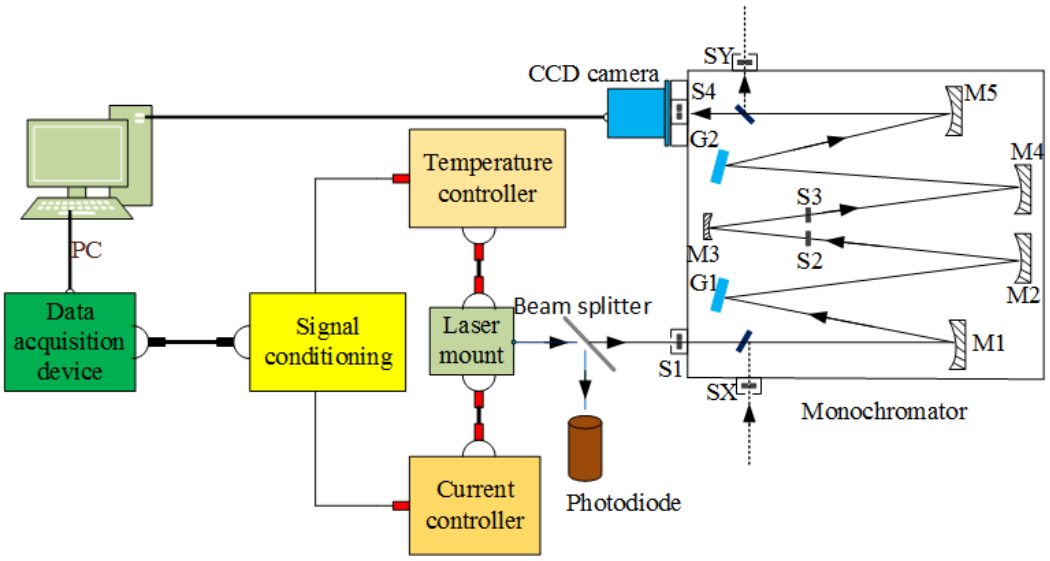

Figure 3.1: An overview of the experimental setup to investigate effects of change in injection current and operating temperature of a GaN based blue laser diode

3.1 Description of the GaN-based Blue Laser Diode

The laser diode studied was LD-445-50PD GaN blue laser diode from Roithner LaserTechnik. The laser diode has emission peak wavelength at 445 nm with output optical power of 50 mW in standard 5.6 mm TO-can package [57]. Figure 3.2 shows a pictorial diagram of used blue laser diode.

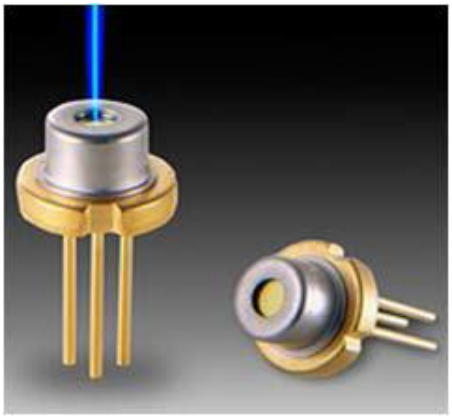

Fig. 3.2: Pictorial diagrams of standard 5. 6 mm TO-can package of blue laser diodes

Table 3.1 shows the operating parameters of employed blue laser diode from Roithner.

Table 3.1: LD-445-50PD GaN blue laser diode specifications [57]

Specification	Min	Typical	Max
Peak wavelength (nm)	440	445	450
Threshold current (mA)	10	35	50
Operating current (mA)	80	120	160
Slope efficiency (W/A)	0.3	0.6	1.0
Operating case temperature (℃)	-10		+60

The blue laser diode was housed in Thorlabs TCLDM9 temperature controlled laser diode mount with an adjustable spherical lens to control beam divergence whenever it is required. Thorlabs LDC 205C current and TED 200C temperature controllers were used to set and monitor the blue laser diode drive current and temperature. TCLDM9 uses thermoelectric coolers to regulate laser diode temperature precisely and its connection with both controllers provides both current regulation and temperature control to 5.6 mm diameter laser diodes. Figure 3.3 shows the pictorial diagram of the connection of the laser diode mount, current and temperature controllers.

Figure 3.3: Pictorial diagram LDC 205C current and TED 200C temperature controller connection with the TCLDM9 laser diode mount.

3.2 Spectrometer and Its Calibration

The laser diode emission spectra were analyzed by a spectrometer which consists of a SPEX 1403 0.85 m double diffraction grating monochromator, with a grating groove density of 1800 grooves/mm, and coupled with the monochromator was an Aphalas CCD-S3600-D(-UV) CCD camera. The calibration of the spectrometer was done with a Krypton lamp. The descriptions and principles of workings of the monochromator and CDD camera are discussed in the first two subsections while the calibration of the spectrometer is presented in the third subsection.

3.2.1 Description and Operation of the Monochromator

The monochromator used is SPEX 1403 0.85 m double grating monochromator with grating density of 1800 grooves/mm which has a high resolution of 0.003 nm. It was used in the experiment to select a wavelength from the available wavelengths in the GaN blue laser diode light. The monochromator is made up of two slits S1 and S2 where the former

is the entrance slit through which light is fed into the monochromator and the latter is the exit slit through which a resolved light is emerged; five mirrors (M1 to M5) to reflect incident light and two reflective diffraction gratings (G1 and G2) to select a wavelength. The wavelength of the emerged light depends on the positions of the gratings. Light enters into the spectrometer through slit S1 and incident on a collimating mirror M1 which reflects off the light onto the diffraction grating G1 where it is dispersed onto a focusing mirror M2. Mirror M2 then reflects off the light towards slit S2 which allows only a narrow wavelength band of the light to pass through and collected by a third mirror M3 which focuses light towards S3 where a narrower wavelength band is allowed to pass through onto a collimating mirror M4. The collimating Mirror M4 directs the light to fall onto the second diffraction grating G2 where it is dispersed onto mirror M5. Finally, M5 reflects the dispersed light towards the exit slit where a light detector (CCD camera) is to be mounted. Mechanism of reflection of light from a grating is shown in Figure 3.4.

3.2.1.1 Diffraction Grating Equation

Figure 3.4 shows a beam of two rays of monochromatic light, R1 and R2 incident on a diffraction grating at an angle θ relative to the normal of the grating. Two rays, R3 and R4, which originates from R1 and R2 got diffracted at a diffraction angle of φ relative to grating normal as depicted in Figure 3.4. The grating is made of grooves which are separated from one another by a distance that is comparable to the wavelength of light under investigation. The path lengths of the two incident and diffracted rays are given as

$$x_1 = d\ \mathrm{Sin}(\theta) \tag{3.1}$$

$$x_2 = d\,\mathrm{Sin}(\varphi) \tag{3.2}$$

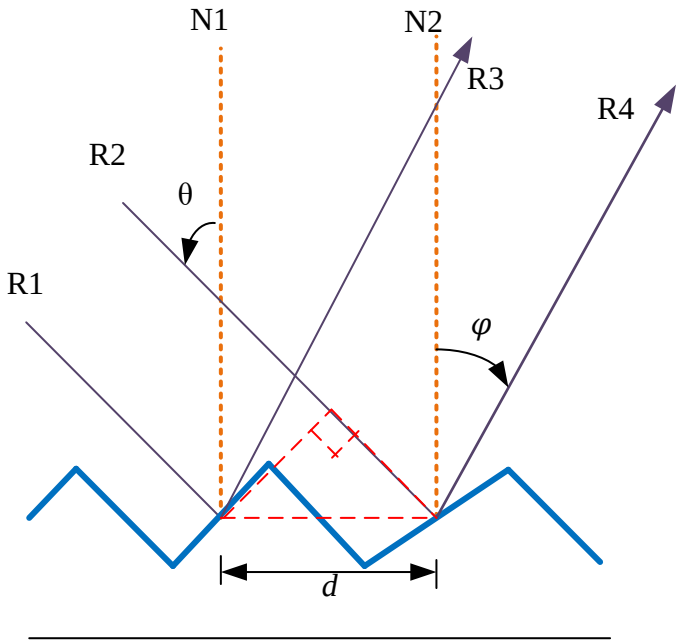

Figure 3.4: Mechanism of diffraction of a beam light from a grating

Then, the overall path difference becomes

$$x = x_1 - x_2 \tag{3.3}$$

$$x = d(\,\mathrm{Sin}\theta + \mathrm{Sin}\varphi)$$

In order to obtain constructive interference, overall path difference must be an integral multiple of the light wavelength $m\lambda$, thus

$$m\lambda = d(\mathrm{Sin}\theta + \mathrm{Sin}\varphi) \tag{3.4}$$

$$Gm\lambda = \mathrm{Sin}\theta + \mathrm{Sin}\varphi \tag{3.5}$$

Equation (3.5) is the diffraction grating equation where $m = \pm(0, 1, 2 \ldots)$ is the grating order, G is the grating groove density which is known as the "groove per millimeter" and as

$$G = \frac{1}{d} \tag{3.6}$$

SPEX 1403 has $G = 1800$ grooves/mm.

By taking the derivative of (3.4) while keeping θ constant,

$$\frac{\mathrm{d}\varphi}{\mathrm{d}\lambda} = \frac{m}{d\ \mathrm{Cos}\varphi} \tag{3.7}$$

where the expression $\mathrm{d}\varphi/\mathrm{d}\lambda$ is the angular dispersion of the grating as a result of a small change in the wavelength of light.

3.2.1.2 Diffraction Grating Resolution

The spectral resolution of the diffraction grating is defined as [58]

$$R = \frac{\lambda}{\delta\lambda} \tag{3.8}$$

or

$$R = \frac{d(\mathrm{Sin}\theta + \mathrm{Sin}\varphi)}{m} \tag{3.9}$$

Equation (3.8) would be used in section 3.2.3 to find the resolution of the spectrometer.

3.2.2 Charge-Coupled Device (CCD) Camera

The CCD camera used in this study is an Alphalas CCD-S3600-D(-UV) with high-sensitivity linear array of 3648 sensor pixels with each pixel having dimensions 8 μm × 200 μm (width × height). It has a spectral range from 320 to 1100 nm [59]. The principle of detection by CCD camera is briefly explained as follows:

CCD is semiconductor device for detecting light/photon in spectroscopy. It is made of several arrays of individual storage units called pixels. Each pixel is made up of several metal-oxide semiconductor (MOS) capacitors where charges are stored. Figure 3.5 shows the schematic diagram of a MOS capacitor. A typical CCD is made from a layer of *n*-doped silicon (Si) built on a *p*-doped Si substrate. The *n*-type Si is covered with a thin, transparent insulating layer of silicon dioxide (SiO_2).

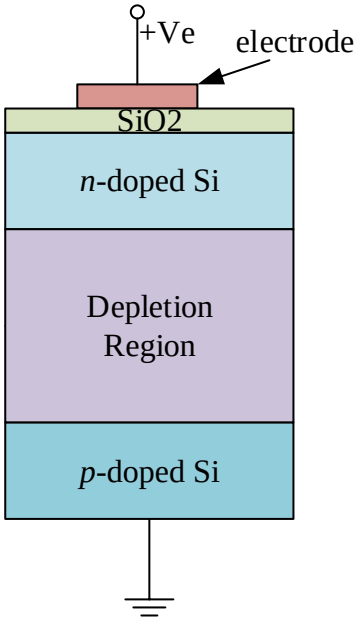

Figure 3.5: Schematic diagram of a MOS capacitor. It represents one storage unit in a CCD camera.

When photons fall on the surface and absorbed by the Si layer, photoelectrons are generated and are collected at the potential well created by a positive voltage applied to the electrode. The amount of photoelectrons depends on the intensity of the light that is absorbed by Si layer. In a CCD where there several number of pixels, after accumulation of charges by the potential wells at the elapse of the exposure time or integration time, the charges are transferred from potential wells to another by changing the applied voltages at the electrodes until they reach the readout stage.

The process of charge transferred is illustrated in Figure 3.6 as follows: each of the pixels has a three-phase electrode (P1, P2 and P3) where every third of the phases is connected together. Movement of the charges is achieved by clock voltages which are applied to the phases and varied.

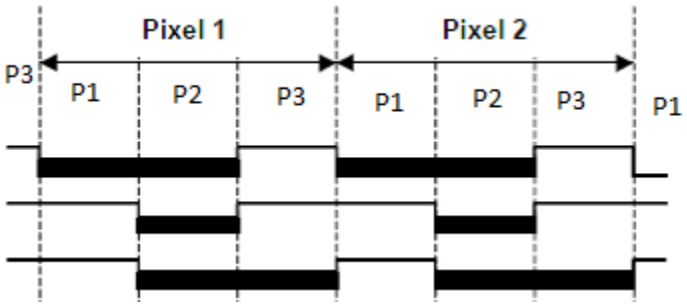

Figure 3.6: Process of transfer of charges among the pixels in CCD

At first, the charges are collected at P1, upon applying a positive voltage at P2, a potential well is created, so the charges are able to occupy the area between P1 and P2. When the voltage at P1 is zero, all the charges are moved completely into P2. Similarly, a potential well is created at P3 on application of a positive voltage, and the well at P2 pours it charges into P3 when the former voltage is made zero. This procedure continues until the charges are moved to where they can be read at the readout register. The charges are converted into electrical signal and amplified by the integrated electronic system in the CCD camera.

CCD quantum efficiency is the fraction of incident photons that generates photoelectrons in the sensor. 100 percent efficiency is not achievable due to some factors such as the incoming photon being reflected back by the electrodes on top of the *n*-doped Si layer. It is also possible that the photons are absorbed by other than the Si layer.

3.2.3 Calibration of the CCD-monochromator System

The CCD was mounted on the monochromator with the aid of a homemade ring extension of diameter 10 cm. The pictorial diagram of the ring is shown in Figure 3.7. Connection of the CCD camera to the PC was done with a USB and the CCD camera software was installed.

Figure 3.7: Ring extension used to mount the CCD to the monochromator exit

Since the laser diode under investigation emits blue light, therefore a lamp that has emission lines in the blue region of the electromagnetic spectrum was employed for calibration. The CCD-Monochromator system was calibrated by using Krypton (Kr) lamp that has three emission lines in the blue region of electromagnetic spectrum, namely 445.391748, 446.369 and 450.235427 nm. The calibration setup for the CCD-monochromator system and the three Kr emission line spectrum are shown in Figure 3.8 and Figure 3.9, respectively.

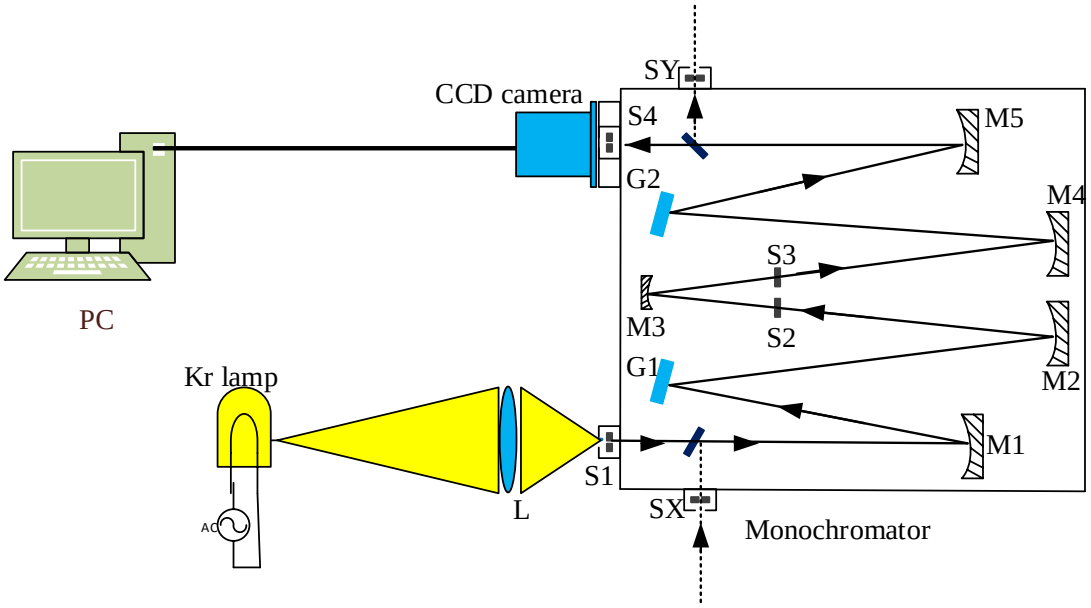

Figure. 3.8: Setup for the calibration of the CCD-Monochromator system

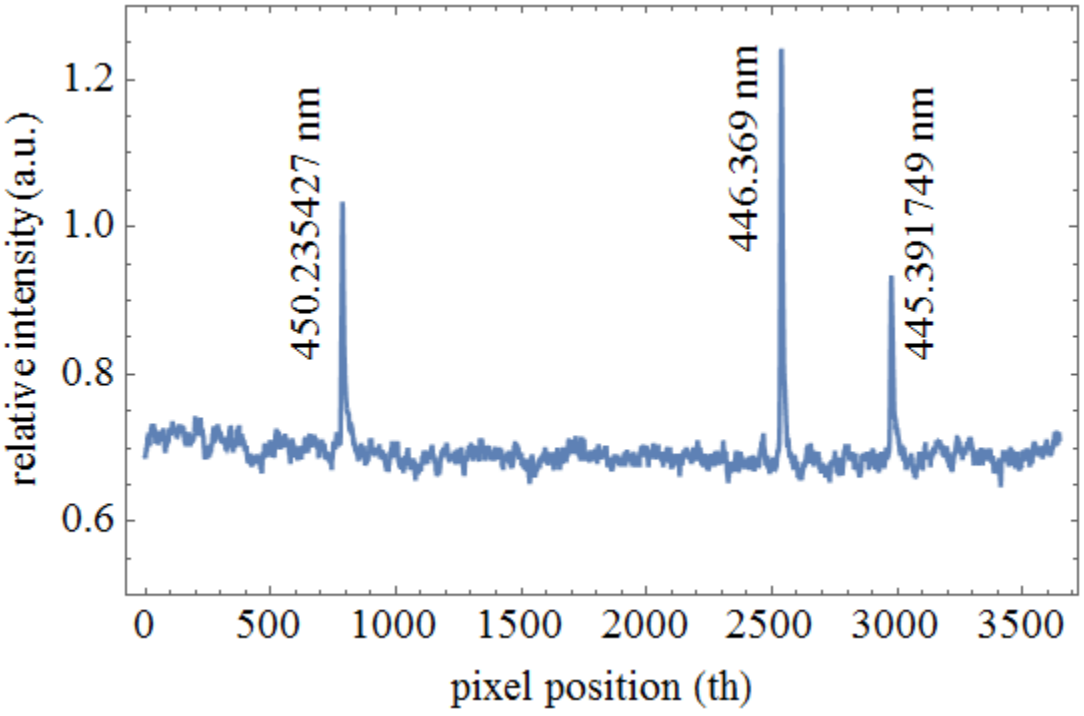

Figure 3.9: Emission spectrum of Krypton lamp with three emission lines

The three Kr emission lines were observed at CCD pixel positions as presented in Table 3.2

Table 3.2: Three Krypton emission lines in the blue region [60]

Pixel position th	Wavelength λ (nm)
2977	445.391748
2539	446.369000
788	450.235427

Figure 3.10 shows the calibration curve obtained from CCD-monochromator system calibration for wavelength. The linear equation (3.10) was obtained for wavelength-pixel relation as

$$\lambda_p = 451.979 - 0.00221142\, p \tag{3.10}$$

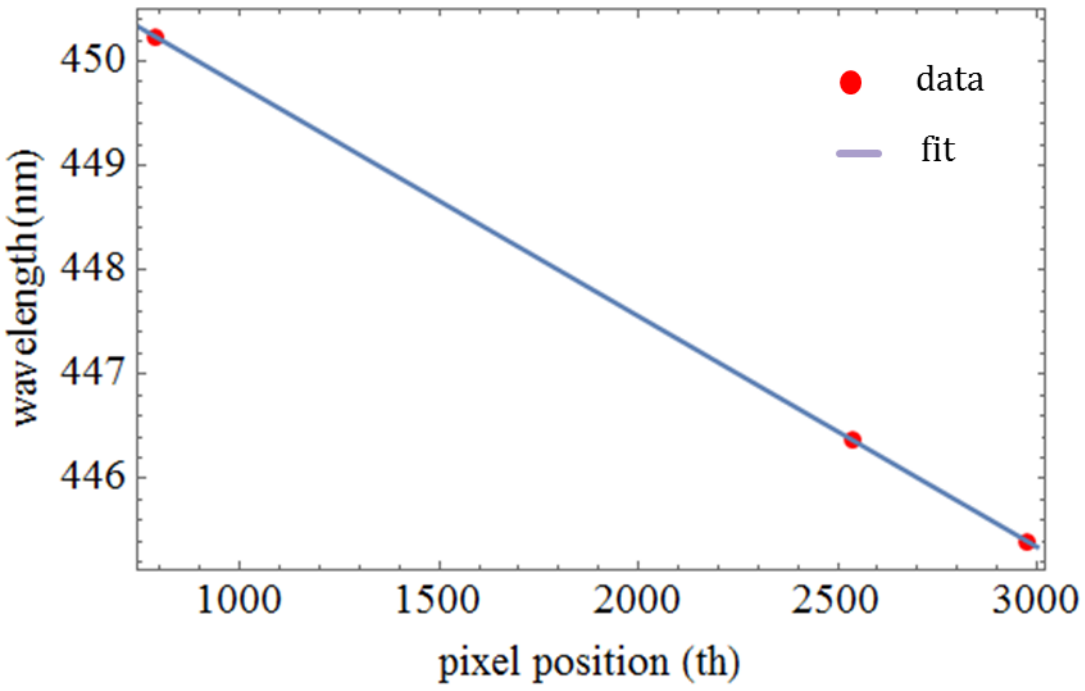

Figure 3.10: Calibration curve for the CCD-monochromator system

The relatively small line slope (0.00221142) of six significant figures and the excellent linear regression ($R^2 = 0.999994$) indicate high level of accuracy in the calibration procedure.

The resolution of the spectrometer is determined by fitting one of the three Kr line peaks in Figure 3.9 to a Lorentzian function in order to obtain the full width at half maximum (FWHM) as shown Figure 3.11.

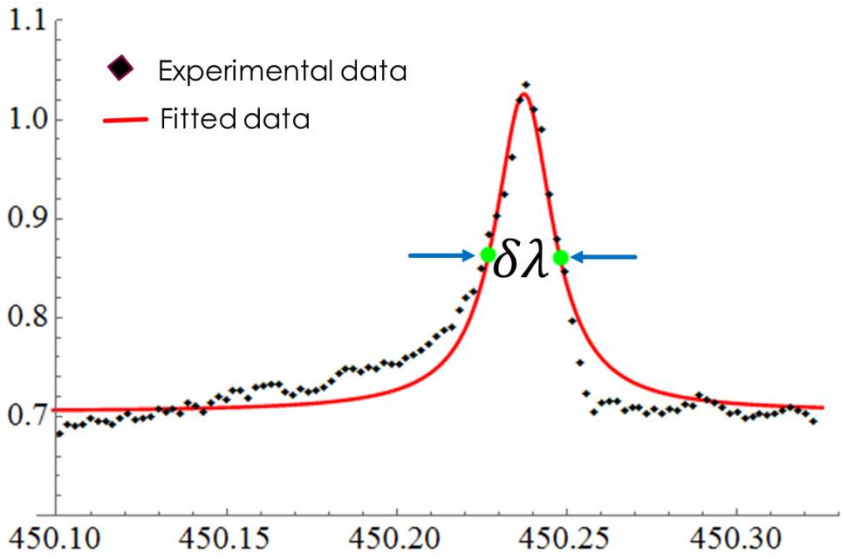

Figure 3.11: Fitting of the Kr lamp line at 788th pixel position

The Lorentzian fit was done for the peak at 788th pixel positon which corresponds to 450.235427 nm. The FWHM contains 9.28542 pixels which gives a linewidth of $\delta\lambda = 0.02$ nm. By using equation (3.8), the resolution of the CCD-monochromator system is evaluated as

$$R = \frac{\lambda}{\delta\lambda} = \frac{450.235427}{0.02}$$

$$R = 21926$$

3.3 Data Acquisition

Having done the required calibrations, the instruments were brought together to build the setup in Fig. 3.1. LabVIEW programs were used for the data acquisitions. The program created a LabVIEW measurement (.lvm) format file which contained the laser diode temperature, injection current, emission spectrum data (pixel positions and intensity) for each of the injection current and temperature values (see Appendix B).

3.3.1 Temporal Stability Study of the GaN-based Blue Laser Diode Output Parameters

Having done the necessary calibrations of the instruments, the different elements of the experiment were brought together as shown in Figure 3.1. The monochromator was used to select wavelength. To investigate the stability of the laser diode output parameters, the laser diode beam divergence was adjusted with the aid of a rotatable spherical lens in the laser diode mount. The laser beam was split into two with the aid of a 50/50 beam splitter; a fraction of the beam was directed to a Thorlabs PDB210A/M photodiode and the other fraction was directed into the monochromator slit with the width set at $8\,\mu m$ (which corresponds to the CCD camera pixel width). The laser diode injection current and temperature were fixed at $100\,mA$ and $20\,℃$ respectively by utilizing the LabVIEW program written for the purpose. The laser diode ran continuously for 10 hours.

3.3.2 Output Optical Measurement of the GaN-based Blue Laser Diode

The laser diode beam was directed into the sensitive area of the PDB210A/M photodiode. The laser diode output optical power was measured for operating temperature range from 5 to $55\,℃$. For each of the set laser diode operating temperature, the injection current into

the laser diode was varied from 0 to 155 mA with an increment of 1 mA. The operating temperature was increased in step of 1 ℃.

3.3.3 Spectral measurement of the GaN based blue laser diode

In this section, the beam splitter was removed and the laser diode mount spherical lens was rotated to make the laser diode beam diverge. This was necessary in order to avoid the effect of beam shift as a result of change in operate temperature while the experiment was going on.

LabVIEW program was used to set and keep the temperature constant at 5 ℃ and the injection current was varied from 0 to 155 mA with an increment of 1 mA. Each time the current was increased to the next value, the program waited for settling time of 4 seconds before it took another spectrum. After taking the last current reading (155 mA) at 5 ℃, the program increased the temperature by 1 ℃, that is, to 6 ℃. The program waited for 60 seconds before it began to inject current from the initial value of 0 and increased it to 155 mA as was done previously. These procedures were repeated for other set temperature points up to 55 ℃ with an increment of 1 ℃. (Each time the temperature was increased by an increment of 1 ℃, the program waited for settling time of 60 seconds before another set of data was collected). The spectra were collected and observed on the PC monitor.

The acquired sets of data obtained were analyzed using Mathematica programs (see Appendix C). The results as well as their discussion are presented in chapter 4 of this thesis.

CHAPTER 4

RESULTS AND DISCUSSION

This chapter presents and discusses the experimental results. Section 4.1 gives the temporal stability of the GaN blue laser diode output, 4.2 discusses the output optical power characteristics, 4.3 discusses the optical gains and 4.4 and 4.5 discuss the effects of temperature and current respectively.

4.1 Temporal Stability of the Output Emissions of the Blue Laser Diode

Figure 4.1 shows the stability of the GaN blue laser diode operated continuously at a constant injection current of 100 mA and operating temperature of 20 ℃ for a period of 9 hours. This is an indication of a good GaN chip structure. There was no noticeable effect of Joule heating of the blue laser diode active layer, thus the operating temperature remained stable at the set value of 20 ℃ despite the high injection current. Owing to the good stability of the injection current and the operating temperature, the output optical power of the GaN blue laser diode was stable. This is an indication that the carrier concentration at the laser diode active layer remained constant for the period the GaN blue laser diode was running. The central lasing wavelength of the GaN blue laser diode emission as depicted did not change as well.

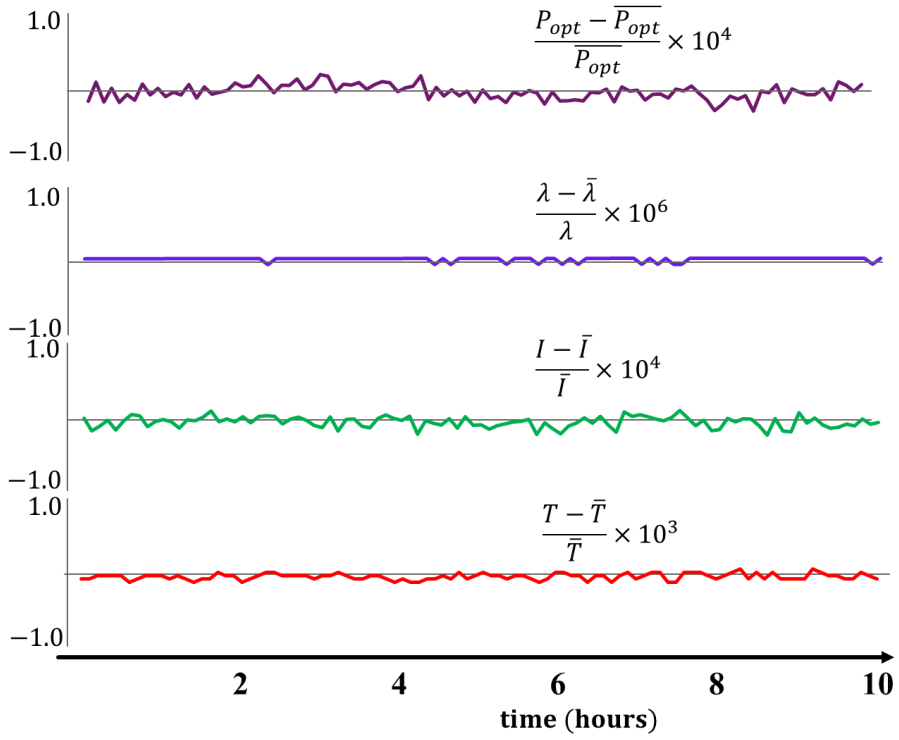

Figure 4.1: Stability of the GaN laser diode parameters for 10 hours at 100 mA and 20 ℃. λ_{cen} is the wavelength of the central peak, I is the injection current, T is the operating temperature and P_{opt} is the output optical power of the GaN blue laser diode. The numbers in the labels were used to scale the actual values of the respective output parameters.

4.2 Output Optical Power characteristics

In order to study the output optical power characteristics, Figure 4.2 shows the 3D plot of output power as a function of injection current and temperature.

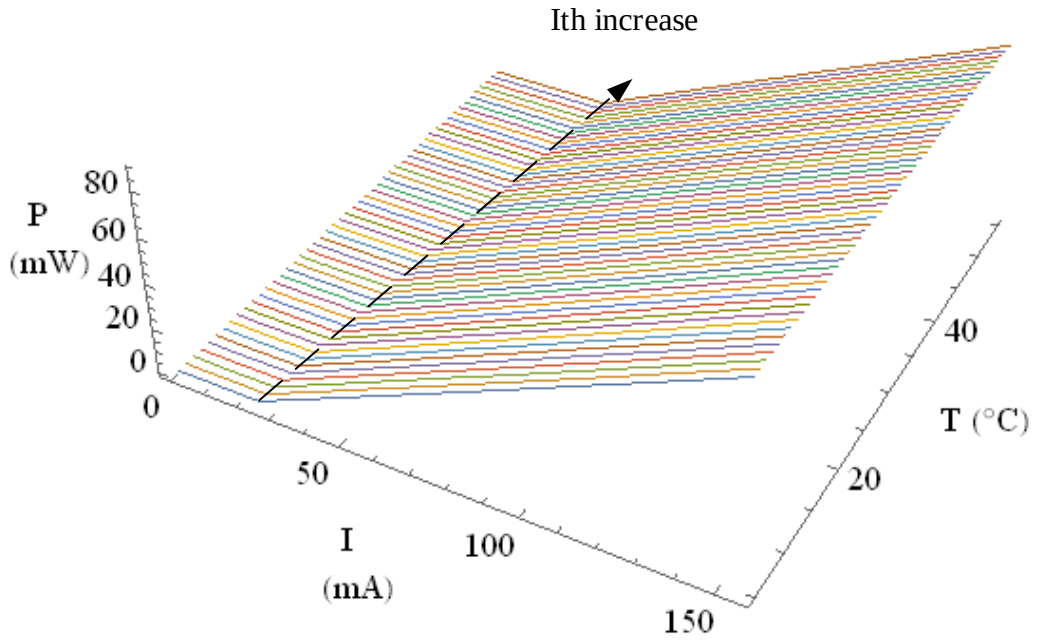

Figure 4.2: Output power (*P*) mW in as a function of current (*I*) in mA and temperature (*T*) in ℃.

The dashed line drawn across the injection current axis shows the trend of how the threshold current of the GaN blue laser diode increased with temperature. This is shown more clearly in the *L-I* curves in Figure 4.3.

The *L-I* curves of the GaN blue laser diode for operating temperatures from 5 to 55 ℃ are shown in Figure 4.3. For each of the laser diode operating temperatures, it was observed that the output optical power slowly increased at injection current below the threshold current, which is an indication of spontaneous emission. As soon as the threshold current was reached and beyond it, the output optical power linearly increased for each of the operating temperatures. The laser diode threshold current increased from 24 mA at 5 ℃ to 36 mA at 55 ℃. The slope efficiency of the laser diode was also observed to decrease as its operating temperature was increased. The increase of the laser threshold current and decrease of its slope efficiency with increase in temperature are attributed to similar loss

mechanism such as undesired reflections at the cleaved end facets, photon absorption by the active and cladding layers, carrier leakage around the active layer.

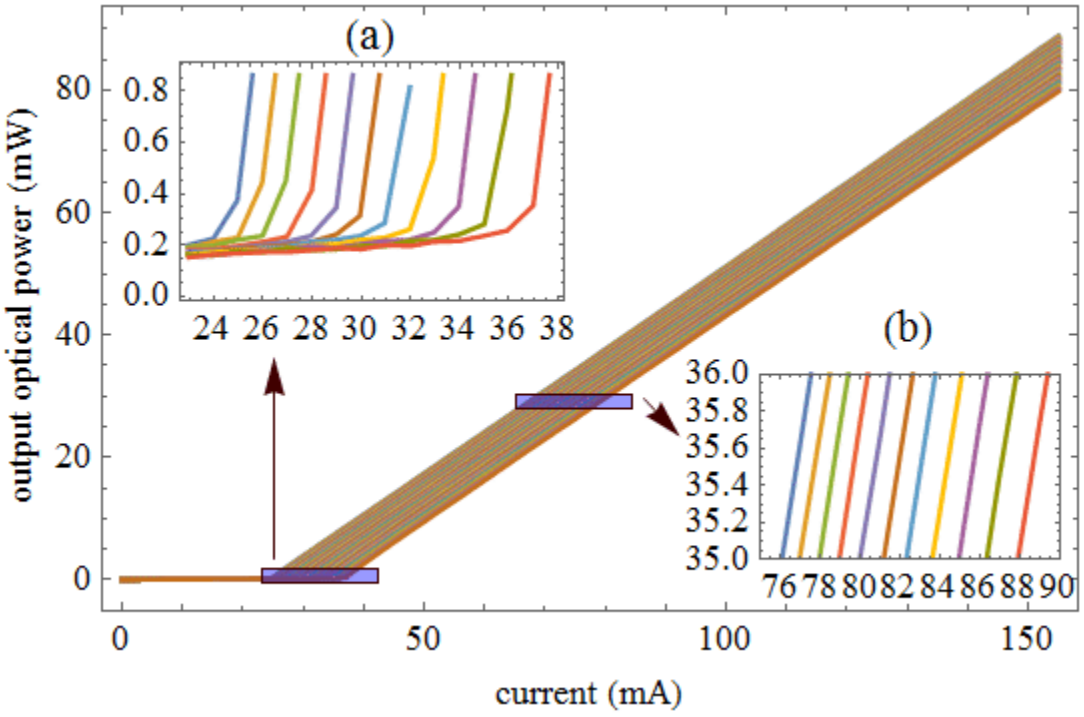

Figure 4.3: $L-I$ curve of the GaN blue laser diode under cw operation for operating temperature from 5 to 55 ℃ in step of 1 ℃ of as a function of temperature. Inset (a) shows eleven *L-I* curves at the onset of lasing for operating temperature from 5 to 55 ℃ in step 5 ℃ where the output optical power started to increase rapidly. Inset (b) shows the same curves at injection current above the threshold current.

When current is injected into a laser diode, part of the injected current flows around the laser diode active layer, this current is known as the leakage current. The leakage current increases with laser diode operating temperature. So more injection current is needed to drive the laser diode into lasing mode at high operating temperature. This therefore shifts the laser diode threshold current to higher values.

Nonradiative recombination and a phenomenon known as Free Carrier Absorption lead to decrease in external differential quantum efficiency. Nonradiative recombination of an

electron and hole generates a phonon instead of a photon that is generated from electron-hole pair radiative recombination. Phonons do not contribute to a laser diode emission. Similarly, free carrier absorption occurs when the laser diode cladding layers absorb the electrons and holes that would have recombined to generate photons. At high temperature, nonradiative recombination and free carrier absorption effects are more pronounced which cause the external differential quantum efficiency to reduce [41].

The external differential quantum efficiency was evaluated for each of the laser diode operating temperature from the slope of the corresponding *L-I* curve by utilizing the derived expression in equation (2.5). The threshold current for each of the operating temperature was also extrapolated from the corresponding *L-I* curve.

Figure 4.4 and Figure 4.5 show the plots of external differential quantum efficiency and threshold current of the blue laser diode as a function of the operating temperature.

The external differential quantum efficiency decreased very slowly with increase in temperature. The insets however show more clearly that there three temperature regimes for the quantum efficiency response to operating temperature. The plot to the right hand-side in inset (a) represents the temperature range between 285 K and 301 K where the external differential quantum efficiency has the highest stability.

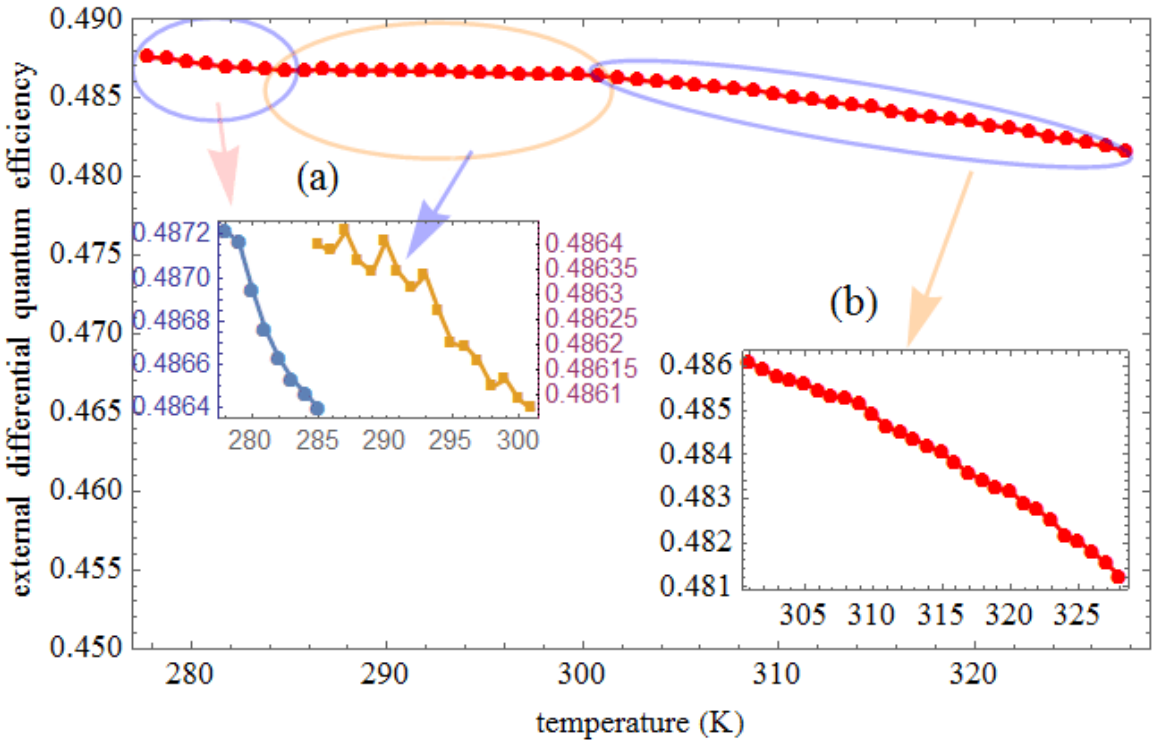

Fig. 4.4: Evaluated external differential quantum efficiency as a function of temperature. Insets (a) and (b) show clearly the three temperature regimes of the quantum efficiency.

The inverse of the slope of the curve of the log of the threshold current plotted against the operating temperature, as shown in Figure 4.5, is the characteristic temperature, T_0 of the laser diode.

$$T_0 = \frac{\Delta T}{\Delta \ln I_{th}} = 130 \text{ K}$$

This characteristic temperature value of the GaN blue laser diode is relatively high [61] for the operating temperature range covered. This is observed in the small change in external differential quantum efficiency with respect to change in operating temperature. However, higher characteristic temperature of GaN blue/violet laser diodes have been reported, [40], [61].

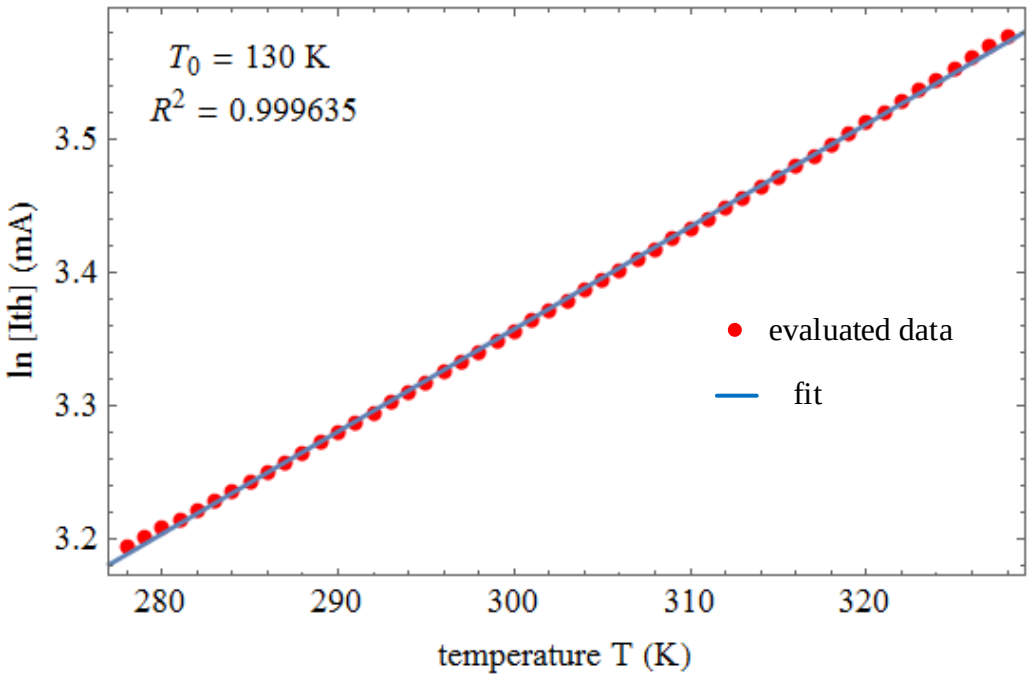

Fig. 4.5: Log of the threshold currents as a function of temperature. The estimated characteristic temperature of the GaN laser diode is 130 K.

The excellent linear regression $R^2 = 0.999635$ indicates the accuracy of the characteristic temperature of the employed laser diode.

4.3 Emission Spectral Output

4.3.1 Gain of the GaN Blue Laser Diode below Threshold Current

Figure 4.6 shows the gain profile of the GaN blue laser diode just before threshold current was reached for 5 ℃, 30 ℃ and 55 ℃. The gain profile shifted to higher wavelengths as temperature was increased. There were already precursors to the nature of longitudinal modes that would be observed while the laser diode would begin to emit coherent emission. Only the modes within the gain region would be amplified during lasing.

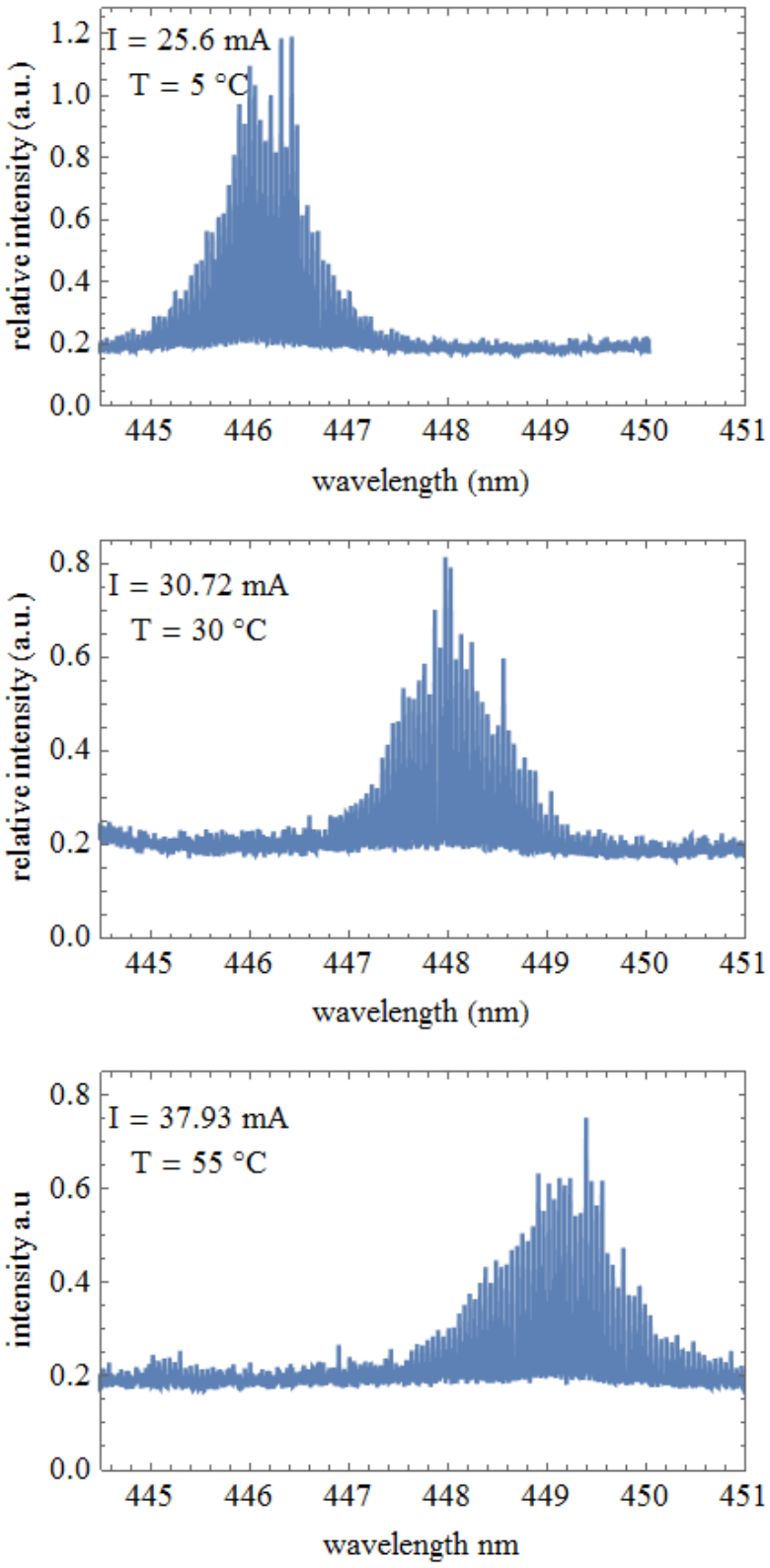

Figure 4.6: Gains of the GaN blue laser diode at injection currents below threshold current at 5 ℃, 30 ℃ and 55 ℃.

4.3.2 Single-mode Emission of the GaN Blue Laser Diode

Figure 4.7 shows the single spectra of the GaN blue laser diode at 5 ℃, 30 ℃ and 55 ℃. These occurred at injection current just above the threshold for each of the three operating temperatures. Since the laser diode is not distributed feedback (DFB) or distributed Bragg reflector (DBR) laser [44], then it is anticipated that if the injection current at each of the laser diode operating temperature that produces a single-mode is increased, other lasing modes would start to appear.

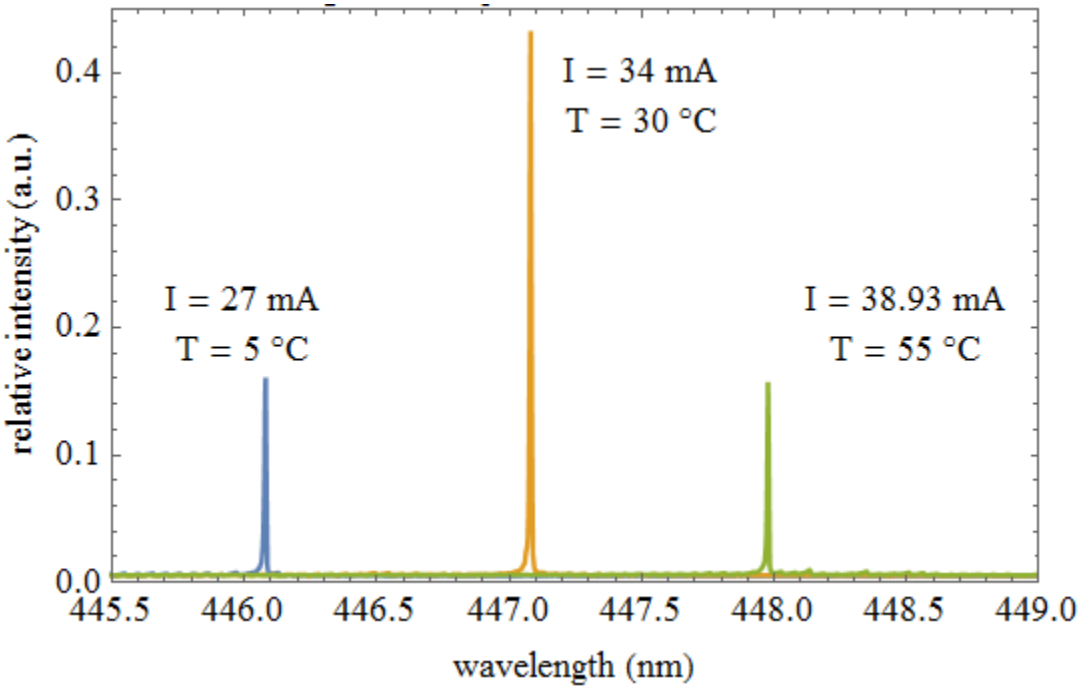

Fig. 4.7: Single-mode emission of the GaN blue laser diode

4.3.3 Emission Spectra well above Threshold Current

Figure 4.8 shows highly resolved spectra of the GaN blue laser diode at 5 ℃, 30 ℃ and 55 ℃ at injection current of 100 mA. Several longitudinal modes were observed with two of mode spacing $\Delta\lambda_1 = 0.0530$ nm and $\Delta\lambda_2 = 0.0550$ nm. These mode spacings are

typical of GaN based blue laser diode, as observed by Romadhon *et al*. [46] and Swietlik *et al*. [62]. The 5 ℃ spectrum has more longitudinal modes than those of 30 ℃ and 55 ℃. Four sub-band emissions were observed for each of the laser diode operating temperatures. Similar sub-band emissions were observed reported by Nakamura *et al* [31] which could attributed to either inhomogeneity of the laser diode active layer or sub-band transitions of quantum energy levels caused by quantum confinement of electrons and holes.

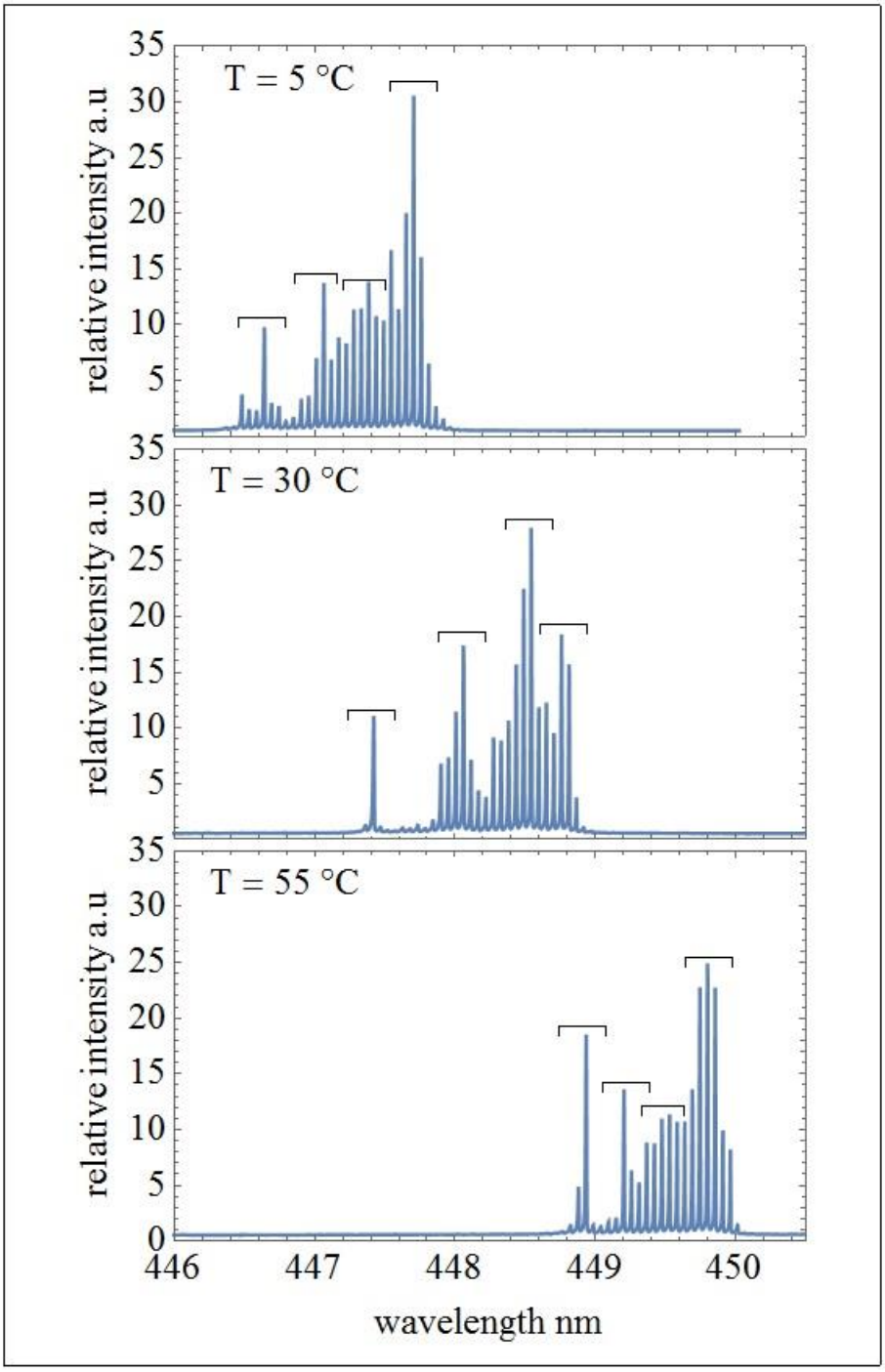

Figure 4.8: Emission spectra of the GaN blue laser diode at 5 ℃, 30 ℃ and 55 ℃ while fixing the injection current at 100 mA. The four bars in each of the plots show four sub-bands in each spectrum.

4.4 Evolution of Optical Gain and Longitudinal Modes

A comparison between experimentally obtained parameters for the evolutions of gain and longitudinal modes in this study and those from literatures is shown in Table 4.1.

Table 4.1: Comparison of optical gain and longitudinal modes evolutions parameters with literature

Parameter	Estimated value	Literature
Current coefficient of longitudinal modes wavelength, $d\lambda_m/dI$ (nm/mA)	0.0059	[a]0.0045 [b]0.0035
Current coefficient of gain wavelength, $d\lambda_g/dI$ (nm/mA)	0.0223	[b]0.023 [c]0.02
Temperature coefficient of longitudinal modes wavelength, $d\lambda_m/dT$ (nm/℃)	0.0149	[a]0.0154
Temperature coefficient of gain wavelength, $d\lambda_g/dT$ (nm/℃)	0.0438	[a]0.0432
Observed mode spacing $\Delta\lambda_1$ (nm) $\Delta\lambda_2$ (nm)	 0.0530 0.0550	[a]0.0548

[a, b, c] see [46]–[48]

4.4.1 Evolution of Optical Gain and Longitudinal Modes due to Change in Injection Current

Figure 4.9 shows the evolution of the laser diode longitudinal modes as a function of change in injection current which was varied from 20 to 155 mA at operating temperatures 5 ℃, 30 ℃ and 55 ℃. When the injection current of the laser diode reached the threshold current and beyond, for each of the operating temperatures, the laser diode emission spectra exhibited multiple longitudinal modes. For of the operating temperatures, the longitudinal mode peak wavelengths were evaluated from the laser diode emission spectra for each injection current, that is, from the threshold current to 155 mA (See Appendix D). Each set of these longitudinal mode peak wavelengths is plotted against its corresponding injection current as shown in Figure 4.9. For the three fixed temperature values, the longitudinal modes peak wavelengths increases linearly with injection current. Increase in injection current causes high carrier concentration at the laser diode active layer. When the injection current is greater than the threshold current, the carrier concentration remains almost constant even though injection current is still being increased. Consequently, Joule heating of the active layer of the laser diode causes its internal temperature to rise. As a result, the physical length (L) of the laser diode active increases, consequently, the longitudinal modes shift to higher wavelengths. Band gap [63] is reduced and refractive index is increased [63] which leads to increase in the active layer optical length (nL). So the overall effect is the shift of the longitudinal modes' wavelengths and the gain peak to higher value. [12]. The lines in the three plots, which are equally spaced and parallel, fit to the observed data points with slope 0.0059 nm/mA. On the other hand, the gain shift was 0.0223 nm/mA. Current coefficients of these orders of magnitudes have also been reported elsewhere [47], [48].

The two slopes show that the gain of the laser diode spectral emission shifts faster than the longitudinal modes. Furthermore, two values of mode spacing observed were 0.0530 nm and 0.0550 nm and are typical for GaN-based blue laser diodes [46].

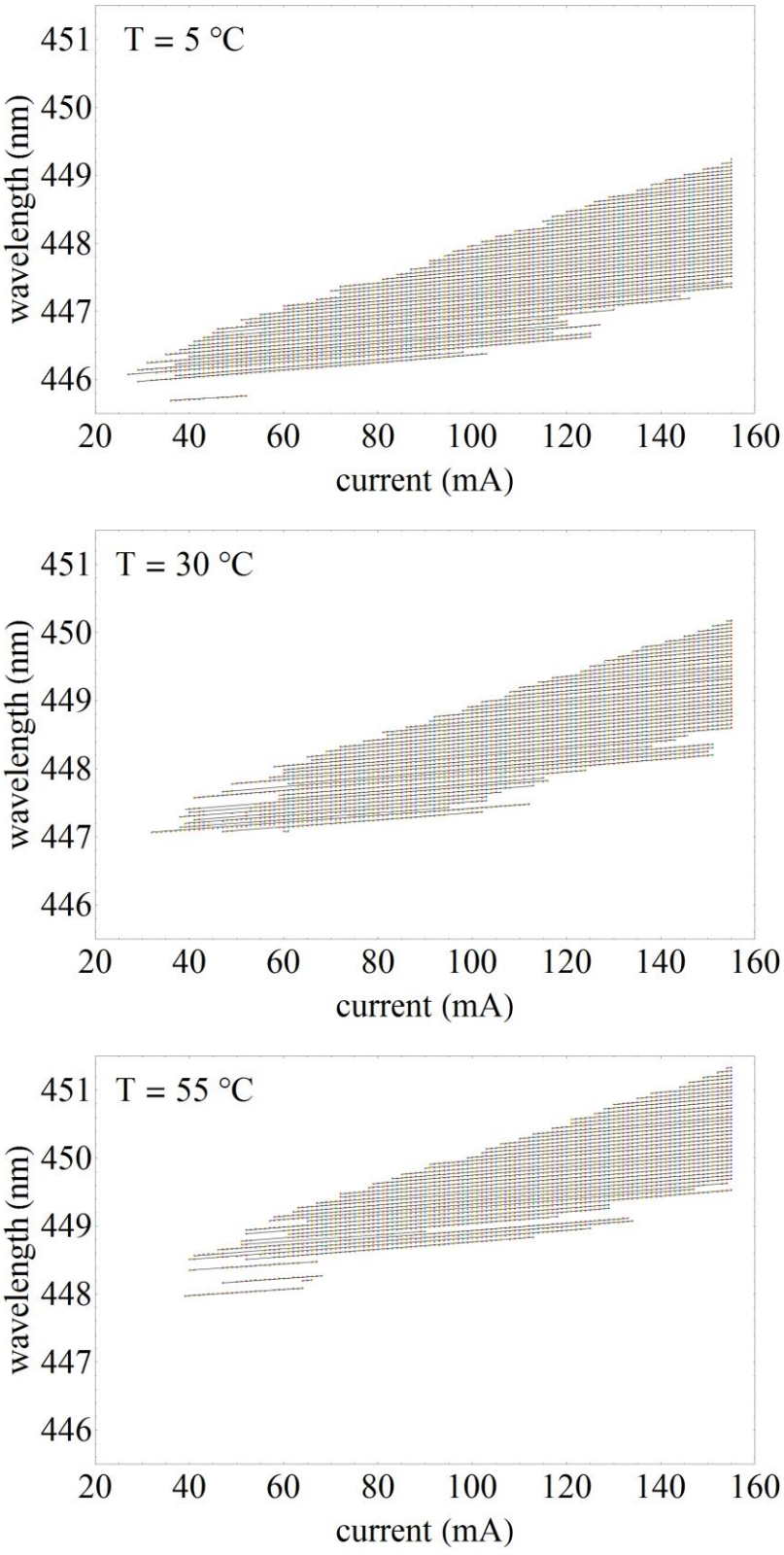

Figure 4.9: Evolution of longitudinal modes as a function of current at 5, 30 and 55 ℃

4.4.2 Evolution of Optical Gain and Longitudinal Modes due to Change in the Laser Diode Operating Temperature

Figure 4.10 shows the evolutions of the laser diode longitudinal modes wavelengths as a function operating temperature which was varied from 5 to 55 ℃ at a fixed injection current of 100 mA. Longitudinal mode peak wavelengths were evaluated from each of the operating temperatures' spectra. Each set of these wavelengths are plotted against its corresponding operating temperature as shown in Figure 4.10. The longitudinal mode wavelengths shifted to longer wavelengths as the operating temperature increased. This is attributed to change in the physical length (L) as well as the effective optical length (nL) of the laser diode active layer. The peak wavelength of the gain profile of the laser diode emission also shifts to longer wavelength with increase in operating temperature. This is attributed to the laser diode active layer band gap reduction as a result of the increase of the laser diode operating temperature. The tracking of the evolution of each of the longitudinal modes' wavelengths with increase in operating temperature of the laser diode was done and fitted to a straight line. The lines are parallel and each one has a slope or temperature coefficient of longitudinal mode wavelength of $0.0149\ \mathrm{nm/℃}$, as shown in Figure 4.10. The longest line in the figure represents the straight line fit for the evolution of the peak wavelength of the laser diode emission gain profile and has slope of $0.0438\ \mathrm{nm/℃}$. The ratio of the temperature coefficient of the gain to that of the longitudinal mode is 2.9 which is comparable to what was obtained by Romadhon *et al* (2.8) [46] and Eichler *et al*. (2.7) [56].

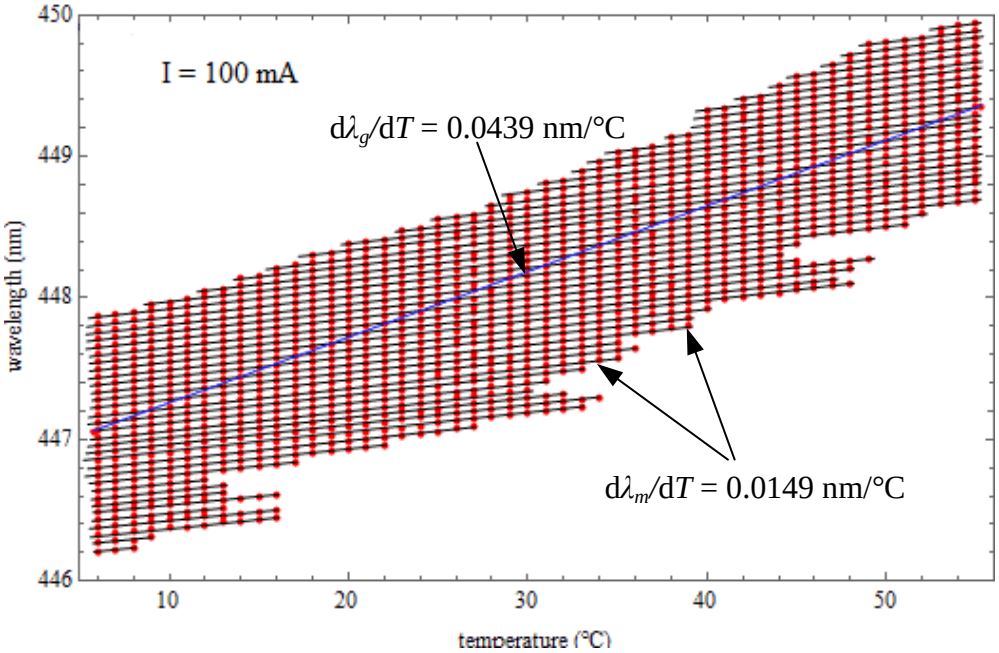

Figure 4.10: Evolution of the laser diode longitudinal modes' wavelengths with variation in its operating temperature while fixing the injection current at 100 mA, where $d\lambda_g/dT$ and $d\lambda_m/dT$ are the temperature coefficient of the gain peak wavelength and longitudinal modes' wavelength respectively.

CHAPTER 5

CONCLUSION

In summary, the emitted longitudinal modes fine spectral substructure of a commercially available GaN-based blue laser diode have been experimentally studied using a high resolution spectroscopic method. Longitudinal modes evolution and temporal stability were investigated by observing sensitivity and behavior of laser diode longitudinal modes emission spectra as a function of applied current and temperature.

In this study, the laser diode outputs that were investigated have good time evolution stability. The laser diode emission wavelength remained highly stable over the running period of 10 hours. The operating temperature of the laser diode was also observed to be stable over the period of time the laser diode was running. These aforementioned qualities are indispensable in spectroscopic applications.

Evolutions of the optical gain and the longitudinal modes of the laser diode as a function of change in injection current at fixed temperature were investigated. In addition to output intensity increase of the modes peaks height, a bathochromic shift for the longitudinal modes was observed to linearly increase upon increasing the laser diode applied current. Current coefficients of the lasing wavelength for the gain and the longitudinal modes estimated were 0.0223 nm/mA and 0.0059 nm/mA, respectively. Similarly, evolution of the optical gain and the longitudinal modes with variations in temperature at fixed injection current revealed that estimated temperature coefficient of the lasing wavelength for the gain was 0.0438 nm/℃ while that of the longitudinal modes was 0.0149 nm/℃. Utilizing emission spectra of longitudinal modes, two values of mode spacing were experimentally

evaluated at 0.0530 nm and 0.0550 nm with percentage of occurrence of 55% and 45%, respectively. These experimental evaluations of mode spacing were found to agree with calculated 0.0530 nm (0.0530 nm) value by incorporating the suitable GaN blue laser cavity parameters. This excellent agreement between experimental and theoretical results lends credence to precision of technique used. The results obtained in this study would serve as a guide for researchers in the field of laser diode spectroscopy.

References

[1] S. Nakamura, M. Senoh, S. Nagahama, N. Iwasa, and T. Yamada, "InGaN-Based Multi-Quantum-Well-Structure Laser Diodes," *Jpn. J. Appl. Phys.*, vol. 35, no. 1B, pp. L74– L76, 1995.

[2] Z. T. Al Dahan, S. Y. Al Dabagh, and A. Assad, "Design and Implementation of Under Water Optical Communication System," *Int. J. Appl. or Innov. Eng. Manag.*, vol. 2, no. 6, pp. 104–109, 2013.

[3] Y. Chi, D. Hsieh, C. Tsai, H. Chen, H. Kuo, and G. Lin, "450-nm GaN laser diode enables high-speed visible light communication with 9-Gbps QAM- OFDM," *Opt. Soceity Am.*, vol. 23, no. 10, pp. 9919–9924, 2015.

[4] A. K. Maini, *Laser Diode Electronics: Fundamentals, Devices and Applications*, 1st edn. John Wiley & Sons, Ltd, 2013.

[5] S. P. Najda, P. Perlin, T. Suski, L. Marona, M. Bockowski, M. Leszczyński, P. Wisniewski, R. Czernecki, R. Kucharski, G. Targowski, S. Watson, and A. E. Kelly, "Advances in AlGaInN laser diode technology," in *SPIE*, 2014, p. 7.

[6] D. Wolff and K. Stolberg, "High Power Diode Lasers and Current Applications," *Laser Tech. J.*, vol. 6, no. 3, pp. 39–43, 2009.

[7] A. A. Bergh, "Blue laser diode (LD) and light emitting diode (LED) Major applications," *Wiley Phys. status solidi*, vol. 2754, no. 12, pp. 2740–2754, 2004.

[8] E. Samsøe, "Laser diode systems for photodynamic therapy and medical

diagnostics," 2004.

[9] M. H. Niemz, *Laser-Tissue Interactions: Fundamentals and Applications*, 3rd ed. Heidelberg: Springer, 2007.

[10] Y. Chi, D. Hsieh, C. Lin, H. Chen, C. Huang, J. He, B. Ooi, S. P. Denbaars, S. Nakamura, H. Kuo, and G. Lin, "Phosphorous Diffuser Diverged Blue Laser Diode for Indoor Lighting and Communication," *Nat. Publ. Gr.*, no. November, pp. 1–9, 2015.

[11] G. Somesfalen, "Environmental Monitoring using Diode-Laser-ased Spectroscopic Techniques," Lund Institute of Technology, 2005.

[12] M. Fukuda, T. Mishima, N. Nakayama, and T. Masuda, "Temperature and current coefficients of lasing wavelength in tunable diode laser spectroscopy," *Appl. Phys. B*, vol. 100, no. 2, pp. 377–382, 2011.

[13] J. T. . Liu, R. K. Hanson, and J. . Jeffries, "High-sensitivity absorption diagnostic for NO2 using a blue diode laser," *J. Quant. Spectrosc. Radiat. Transf.*, vol. 72, pp. 655–664, 2002.

[14] H. P. Maruska and J. J. Tietjen, "The preparation and properties of vapor-deposited single-crystal-line GaN," *Appl. Phys. Lett.*, vol. 15, no. 10, pp. 327–329, 1969.

[15] H. P. Maruska, W. C. Rhines, and D. a. Stevenson, "Preparation of Mg-doped GaN diodes exhibiting violet electroluminescence," *Mater. Res. Bull.*, vol. 7, no. 8, pp.

777–781, 1972.

[16] R. N. Hall, G. E. Fenner, J. D. Kingsley, T. J. Soltys, and R. O. Carlson, “Coherent light emission from GaAs junctions,” *Phys. Rev. Lett.*, vol. 9, no. 9, pp. 366–368, 1962.

[17] J. I. Pankove, J. E. Berkeyheiser, H. P. Maruska, and J. Wittke, “Luminescent properties of GaN,” *Solid State Commun.*, vol. 8, no. 13, pp. 1051–1053, 1970.

[18] J. I. Pankove, M. T. Duffy, E. a. Miller, and J. E. Berkeyheiser, “Luminescence of insulating Be-doped and Li-doped GaN,” *J. Lumin.*, vol. 8, no. 1, pp. 89–93, 1973.

[19] J. I. Pankove and J. E. Berkeyheiser, “Properties of Zn-doped GaN. II. Photoconductivity,” *J. Appl. Phys.*, vol. 45, no. 9, pp. 3892–3895, 1974.

[20] J. I. Pankove, E. a. Miller, and J. E. Berkeyheiser, “GaN blue light-emitting diodes,” *J. Lumin.*, vol. 5, no. 1, pp. 84–86, 1972.

[21] J. I. Pankove, E. a. Miller, D. Richman, and J. E. Berkeyheiser, “Electroluminescence in GaN,” *J. Lumin.*, vol. 4, no. 1, pp. 63–66, 1971.

[22] H. P. Maruska, D. a. Stevenson, and J. I. Pankove, “Violet luminescence of Mg-doped GaN,” *Appl. Phys. Lett.*, vol. 22, no. 6, pp. 303–305, 1973.

[23] A. J. Nelson, C. R. Schwerdtfeger, S.-H. Hei, A. Zunger, D. Rioux, R. Patel, and H. Hochst, “Theoretical and experimental studies of the ZnSe/CuInSe2 heterojunction and band offset,” vol. 2557, no. 1993, pp. 12–15, 1996.

[24] H. Okuyama, T. Miyajama, Y. Morinaga, F. Hiei, M. Ozawa, and K. Akimoto,

"ZnSe/ZnMgSSe blue laser diode," *Inst. Eng. Technol.*, vol. 28, no. 19, pp. 1798–1799, 1992.

[25] C. Boney, Z. Yu, W. H. Rowland, W. C. Hughes, J. W. Cook, J. F. Schetzina, G. Cantwell, and W. C. Harsch, "II – VI blue / green laser diodes on ZnSe substrates," *J. Vac. Sci. Technol. B*, vol. 14, no. 3, pp. 2259–2262, 1996.

[26] H. Amano, M. Kito, K. Hiramatsu, and I. Akasaki, "p-Type Conduction in Mg-Doped GaN Treated with Low-Energy Electron Beam Irradiation (LEEBI)," *Jpn. J. Appl. Phys.*, vol. 28, no. 12, pp. L2112–L2114, 1989.

[27] S. Nakamura, T. Mukai, and M. Senoh, "High-Power GaN P-N Junction Blue-Light-Emitting Diodes," *Jpn. J. Appl. Phys.*, vol. 30, no. 12A, p. L 1998–L 2001, 1991.

[28] G. Karczewski, "Gallium nitride - The prospective winner of the blue-laser competition?," *Opto-Electronic Rev.*, vol. 5, no. 1, pp. 59–62, 1997.

[29] S. Nakamura, "InGaN-based blue laser diodes," *IEEE J. Sel. Top. Quantum Electron.*, vol. 3, no. 3, pp. 712–718, 1997.

[30] S. Kasap and P. Capper, *Springer Handbook of Electronic and Photonic Materials*. Springer Science and Business Media, 2007.

[31] S. Nakamura, S. Pearton, and G. Fasol, *The Blue Laser Diode: The Complete Story*, Second. Berlin, Heidelberg: Springer-Verlag Berlin Heidelberg GmbH, 2000.

[32] H. Nasim and Y. Jamil, “Diode lasers: From laboratory to industry,” *Opt. Laser Technol.*, vol. 56, pp. 211–222, 2014.

[33] J. Singh, *Electronic and Optoelectronic Properties of Semiconductor Structures*. Cambridge: Cambridge University Press, 2003.

[34] S. M. Thahab, H. A. Hassan, and Z. Hassan, “Performance of InGaN/GaN Laser Diode Based on Quaternary Alloys Stopper and Superlattice Layers,” *World Acad. Sci. Eng. Technol.*, vol. 55, no. 7, pp. 11–15, 2009.

[35] H. Sun, *Laser Diode Beam Basics, Manipulations and Characterizations*. New York: Springer, 2012.

[36] H. Morkoç, *Handbook of Nitride Semiconductors and Devices , GaN-based Optical and Electronic Devices*. John Wiley & Sons, 2009.

[37] N. Ainslie, M. Pilkuhn, and H. Rupprecht, “High-Energy Light Emission from Junctions in GaAs x P1 − x Diodes,” *J. Appl. Phys.*, vol. 35, no. 1, pp. 105–107, 1964.

[38] O. Svelto, *Principles of Lasers*, Fifth edn. Springer, 2010.

[39] R. Diehl, *High-Power Diode Lasers: Fundamentals, Technology, Applications*. Berlin Heidelberg: Springer-Verlag, 2000.

[40] W. G. Scheibenzuber, “GaN-Based Laser Diodes: Towards Longer Wavelengths and Short Pulses,” Fraunhofer Institute for Applied Solid State Physics, 2012.

[41] T. Numai, *Fundamentals of Semiconductor Lasers*, 2nd edn. Tokyo: Springer

Tokyo, 2015.

[42] K. Petermann, *Laser Diode Modulation and Noise*, 1st edn. Dordrecht: Kluwer Academic Publishers, 1988.

[43] H. Zappe, *Laser Diode Microsystems*, First. Berlin Heidelberg: Springer-Verlag Berlin Heidelberg, 2004.

[44] K. Thyagarajan and A. Ghatak, *Lasers Fundamentals and Applications*, 2nd edn. New Delhi: Springer, 2010.

[45] M. Fukuda, *Optical Semiconductor Devices*. New York: John Wiley & Sons, 1999.

[46] M. S. Romadhon, A. Aljalal, W. Al-Basheer, and K. Gasmi, "Longitudinal modes evolution of a GaN-based blue laser diode," *Opt. Laser Technol.*, vol. 70, pp. 59–62, 2015.

[47] T. Meyer, H. Braun, U. T. Schwarz, M. Schillgalies, S. Lutgen, and U. Strauss, "Spectral dynamics of 405 nm (Al , In) GaN laser diodes grown on GaN and SiC substrate," *Opt. Express*, vol. 16, no. 10, pp. 6833–6845, 2008.

[48] G. Ropars, a. Le Floch, and G. P. Agrawal, "Spectral and spatial dynamics in InGaN blue-violet lasers," *Appl. Phys. Lett.*, vol. 89, no. 24, pp. 129–131, 2006.

[49] T. Higashi, T. Yamamoto, S. Ogita, and M. Kobayashi, "Experimental Analysis of Temperature Dependence of Oscillation Wavelength in Quantum-Well FP Semiconductor Lasers," *IEEE J. Quantum Electron.*, vol. 34, no. 9, pp. 1680–1689, 1998.

[50] D. Sand, *Diode Lasers: Series in Optics and Optoelectronics*, First. Bristol & Philadelphia: Institute of Physics Publishing Ltd, 2005.

[51] J. I. Pankove, “Temperature Dependence of Emission Efficiency and Lasing Threshold in Laser Diodes,” *IEEE J. Quantum Electron.*, vol. 4, no. 4, pp. 119–122, 1968.

[52] H. Jiang, “III-Nitride Semiconductors: Optical Properties,” CRC Press, 2002.

[53] U. Tisch, B. Meyler, O. Katz, E. Finkman, J. Salzman, U. Tisch, B. Meyler, O. Katz, E. Finkman, and J. Salzman, “Dependence of the refractive index of Al x Ga 1 − x N on temperature and composition at elevated temperatures Dependence of the refractive index of Al x Ga 1 À x N on temperature and composition at elevated temperatures,” *J. Appl. Phys.*, vol. 89, no. 5, pp. 2676–2685, 2001.

[54] N. Antoine-Vincent, F. Natali, M. Mihailovic, A. Vasson, J. Leymarie, P. Disseix, D. Byrne, F. Semond, and J. Massies, “Determination of the refractive indices of AlN , GaN , and Al x Ga 1 − x N grown on (111) Si substrates Determination of the refractive indices of AlN , GaN , and Al x Ga 1 À x N grown on „ 111 … Si substrates,” *J. Appl. Phys.*, vol. 93, no. 9, pp. 5222–5226, 2003.

[55] N. Watanabe, T. Kimoto, and J. Suda, “The temperature dependence of the refractive indices of GaN and AlN from room temperature up to 515 ° C The temperature dependence of the refractive indices of GaN and AlN from room temperature up to 515 ° C,” *J. Appl. Phys.*, vol. 104, no. 10, pp. 1061011–1061013, 2008.

[56] C. Eichler, S. S. Schad, F. Scholz, D. Hofstetter, S. Miller, A. Weimar, A. Lell, and V. Härle, “Observation of temperature-independent longitudinal-mode patterns in violet-blue InGaN-based laser diodes,” *IEEE Photonics Technol. Lett.*, vol. 17, no. 9, pp. 1782–1784, 2005.

[57] Roithner, “LASER DIODES - UV LASER DIODES - VIOLET LASER DIODES - BLUE,” 2016.

[58] C. Palmer, *Diffraction Grating Handbook*, 6 ed. New York: Newport Corporation, 2005.

[59] Alphalas, “Advanced High-Speed Digital CCD Line Camera CCD-S3600-D(-UV),” 2014.

[60] E. B. Saloman, “Energy Levels and Observed Spectral Lines of Krypton , Kr I through Kr XXXVI,” *J. Phys. Chem. Ref. Data*, vol. 36, no. 1, 2007.

[61] T. Świetlik, G. Franssen, P. Wiśniewski, S. Krukowski, S. P. Łepkowski, L. Marona, M. Leszczyński, I. Grzegory, T. Suski, S. Porowski, P. Perlin, and R. Czernecki, “Anomalous temperature characteristics of single wide quantum well InGaN laser diode,” *Appl. Phys. Lett.*, vol. 88, no. 071121, pp. 26–29, 2006.

[62] T. Swietlik, G. Franssen, R. Czernecki, M. Leszczynski, C. Skierbiszewski, I. Grzegory, T. Suski, P. Perlin, C. Lauterbach, and U. T. Schwarz, “Mode dynamics of high power (InAl)GaN based laser diodes grown on bulk GaN substrate,” *J. Appl. Phys.*, vol. 101, no. 8, pp. 0831091–0831096, 2007.

[63] C. Bulutay, C. M. Turgut, and N. A. Zakhleniuk, “Carrier-induced refractive index change and optical absorption in wurtzite InN and GaN: Fullband approach,” *Condens. Matter Mater. Sci. J.*, pp. 1–10, 2010.

Appendix A

Front panel of the LabVIEW program used to acquire and store experimental data

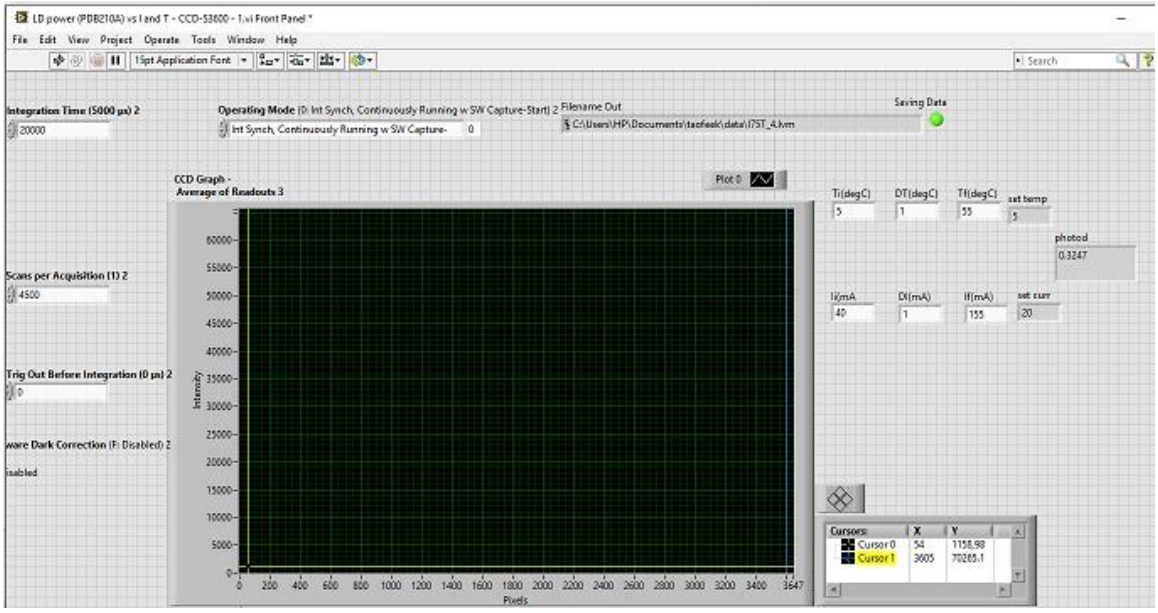

Appendix B

A sample of the format of the arrangement of the experimental data stored in LabVIEW measurement (.lvm) files.

LabVIEW Measurement					
Writer_Version	2				
Reader_Version	2				
Separator	Tab				
Decimal_Separator	.				
Multi_Headings	Yes				
X_Columns	One				
Time_Pref	Relative				
Operator	HP				
Date	########				
Time	42:12.1				
End_of_Header					
Notes	X values guaranteed valid only for Untitled				
Channels	3				
Samples	3648	3648	3648		
Date	########	########	########		
Time	42:15.8	42:12.1	42:12.1		
Y_Unit_Label		Volts	Volts		
X_Dimension	Time	Time	Time		
X0	0.00E+00	0.00E+00	0.00E+00		
Delta_X	1	0.001	0.001		
End_of_Header					
X_Value	Untitled	vCurrOut	vTempOut	Comment	
0	509	-0.00367	0.247188		
1	508	-0.00335	0.246542		
2	513	-0.00367	0.246542		
…	…	…	…		
…	…	…	…		
3647	514	-0.00302	0.247188		

Appendix C

Mathematica program used to analyze data acquired by the LabVIEW programs

```
SetDirectory[NotebookDirectory[]];
SetOptions[{ListPlot, ListLinePlot, ListPlot3D, ListPointPlot3D, Plot},
BaseStyle → {FontFamily → "Times", FontSize → 12}, LabelStyle → {Black, Black}];
imin = 1; imax = 156;
LISTWAVELENGTHVSINTENSITY = {};
HIGHESTPEAK = {}
PIXELHIGHESTPEAK = {};
WAVELENGTHOFHIGHESTPEAK = {};
LISTWAVELENGTHCURRENTINTENSITY = {};
INTENSITY = {}; CURRENT = {}; TEMPERATURE = {};
FINDPEAKS = {};
SELECTPEAKS = {};
LENGTHSELECTPEAKS = {};
PLOTSELECTPEAKS = {};
WAVELENGTHOFPEAKS = {};
MODESPACING = {};
LISTMODESPACINGPERSPEC = {};
LENGTHWAVELENGTHOFPEAKS = {};
WAVELENGTHVSCURRENT = {};
For[i = imin, i ≤ imax, i++, or = OpenRead["TI_" <> ToString[i] <> ".lvm"];
rl = ReadList[or, Record];
ss = StringSplit[rl];
te = Table[ToExpression[ss[[i]]], {i, 26, Length[ss]}];
list1 = Table[{0.995685 (451.979 - 0.00221142 te[[i, 1]]), te[[i, 2]],
50.408 te[[i, 3]] + 0.181, 20.409 te[[i, 4]] - 0.0222}, {i, 1, Length[te]}]
(*list1 = wavelength, intensity, current, temperature*);
listwavelengthvsintensity =
Table[{0.995685 (451.979 - 0.00221142 te[[i, 1]]), te[[i, 2]] / 1000},
{i, 1, Length[te]}];
list2 = Table[{0.995685 (451.979 - 0.00221142 te[[i, 1]]),
50.408 te[[i, 3]] + 0.181, te[[i, 2]] / 1000}, {i, 1, Length[te]}]
(*list2 = wavelength, current, intensity*);
intensity = Table[te[[i, 2]] / 1000, {i, 1, Length[te]}];
highestpeak = Max[intensity];
pixelhighestpeak = Position[intensity, highestpeak][[1, 1]];
wavelengthofhighestpeak = 0.995685 (451.979 - 0.00221142 pixelhighestpeak);
current = Mean[Table[50.408 te[[i, 3]] + 0.181, {i, 1, Length[te]}]];
temperature = Mean[Table[20.409 te[[i, 4]] - 0.0222, {i, 1, Length[te]}]];
findpeaks = FindPeaks[intensity, 6];
selectpeaks = Select[findpeaks, Last[#] > 0.700 &];
lengthselectpeaks = Length[selectpeaks];
plotselectpeaks = ListLinePlot[intensity,
```

```
Epilog → {Red, PointSize[0.01], Point[selectpeaks(*[[]]*)]}, Frame → True,
FrameLabel → {"pixel position (th)", "relative intensity (a.u.)"},
PlotRange → {{00, 2900}, {0, 35}}];
wavelengthofpeaks = Table[0.995685 (451.979 - 0.00221142 selectpeaks[[i, 1]]),
{i, 1, Length[selectpeaks]}];
modespacing = 0.995685 × 0.00221142
(selectpeaks[[12]][[1]] - selectpeaks[[11]][[1]]);
listmodespacingperspec = 0.995685 × 0.00221142
Differences[Table[selectpeaks[[i, 1]], {i, 1, Length[selectpeaks]}]];
lengthwavelengthofpeaks = Length[wavelengthofpeaks];
wavelengthvscurrent =
Transpose[{ConstantArray["" <> ToString[i - imin] <> "", lengthwavelengthofpeaks],
wavelengthofpeaks}];
LISTWAVELENGTHVSINTENSITY =
Append[LISTWAVELENGTHVSINTENSITY, listwavelengthvsintensity];
HIGHESTPEAK = Append[HIGHESTPEAK, highestpeak];
PIXELHIGHESTPEAK = Append[PIXELHIGHESTPEAK, pixelhighestpeak];
WAVELENGTHOFHIGHESTPEAK =
Append[WAVELENGTHOFHIGHESTPEAK, wavelengthofhighestpeak];
LISTWAVELENGTHCURRENTINTENSITY =
Append[LISTWAVELENGTHCURRENTINTENSITY, list2];
INTENSITY = Append[INTENSITY, intensity];
CURRENT = Append[CURRENT, current];
TEMPERATURE = Append[TEMPERATURE, temperature];
FINDPEAKS = Append[FINDPEAKS, findpeaks];
SELECTPEAKS = Append[SELECTPEAKS, selectpeaks];
LENGTHSELECTPEAKS = Append[LENGTHSELECTPEAKS, lengthselectpeaks];
PLOTSELECTPEAKS = Append[PLOTSELECTPEAKS, plotselectpeaks];
WAVELENGTHOFPEAKS = Append[WAVELENGTHOFPEAKS,
wavelengthofpeaks];
MODESPACING = Append[MODESPACING, modespacing];
LISTMODESPACINGPERSPEC =
Append[LISTMODESPACINGPERSPEC, listmodespacingperspec];
2 copy to word appendix.nb
LENGTHWAVELENGTHOFPEAKS =
Append[LENGTHWAVELENGTHOFPEAKS, lengthwavelengthofpeaks];
WAVELENGTHVSCURRENT = Append[WAVELENGTHVSCURRENT,
wavelengthvscurrent];
]
```

Appendix D

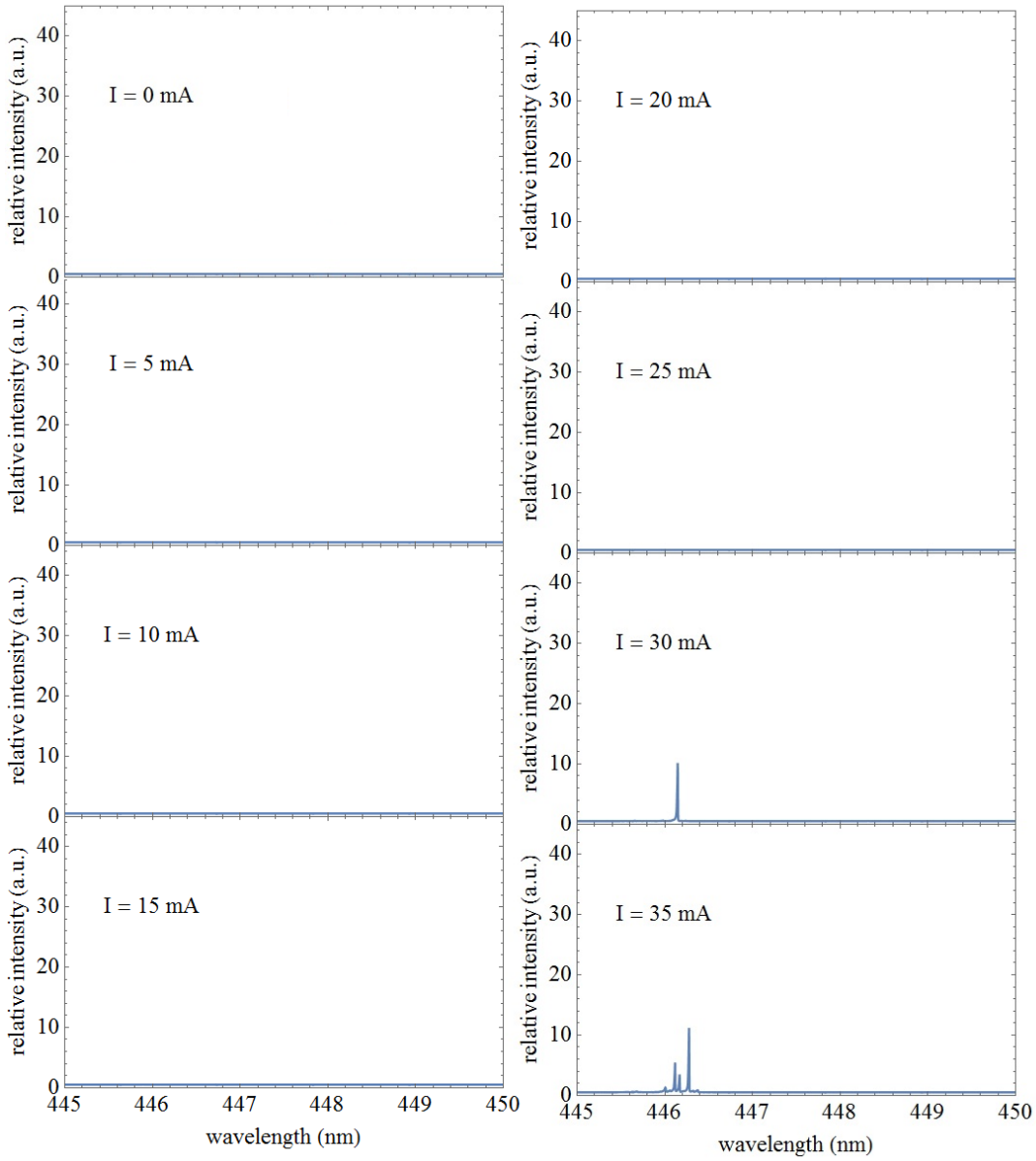

Figure D1: Emission spectra of the GaN blue laser diode at 5 ℃

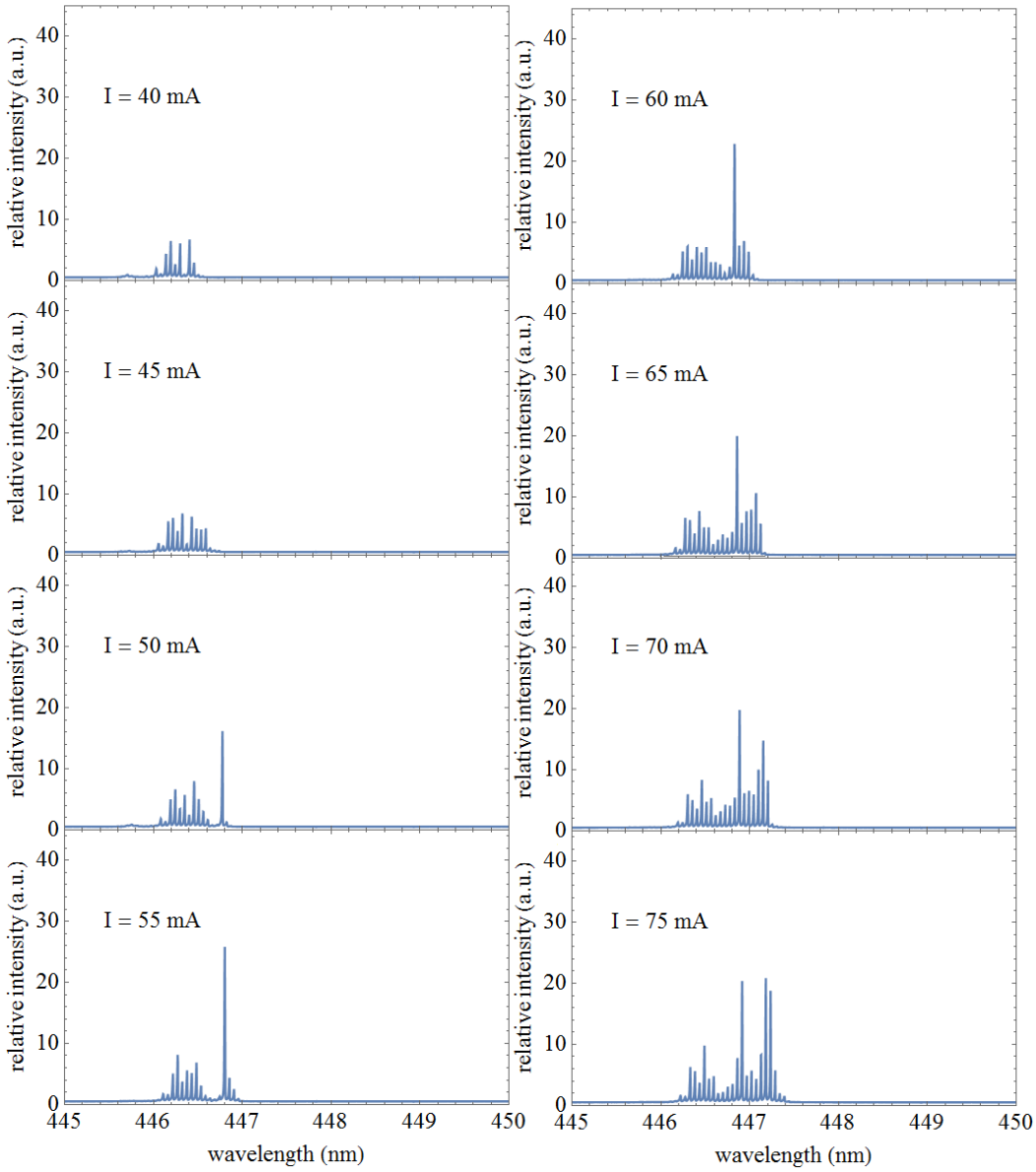

Figure D2: Emission spectra of the GaN blue laser diode at 5 ℃

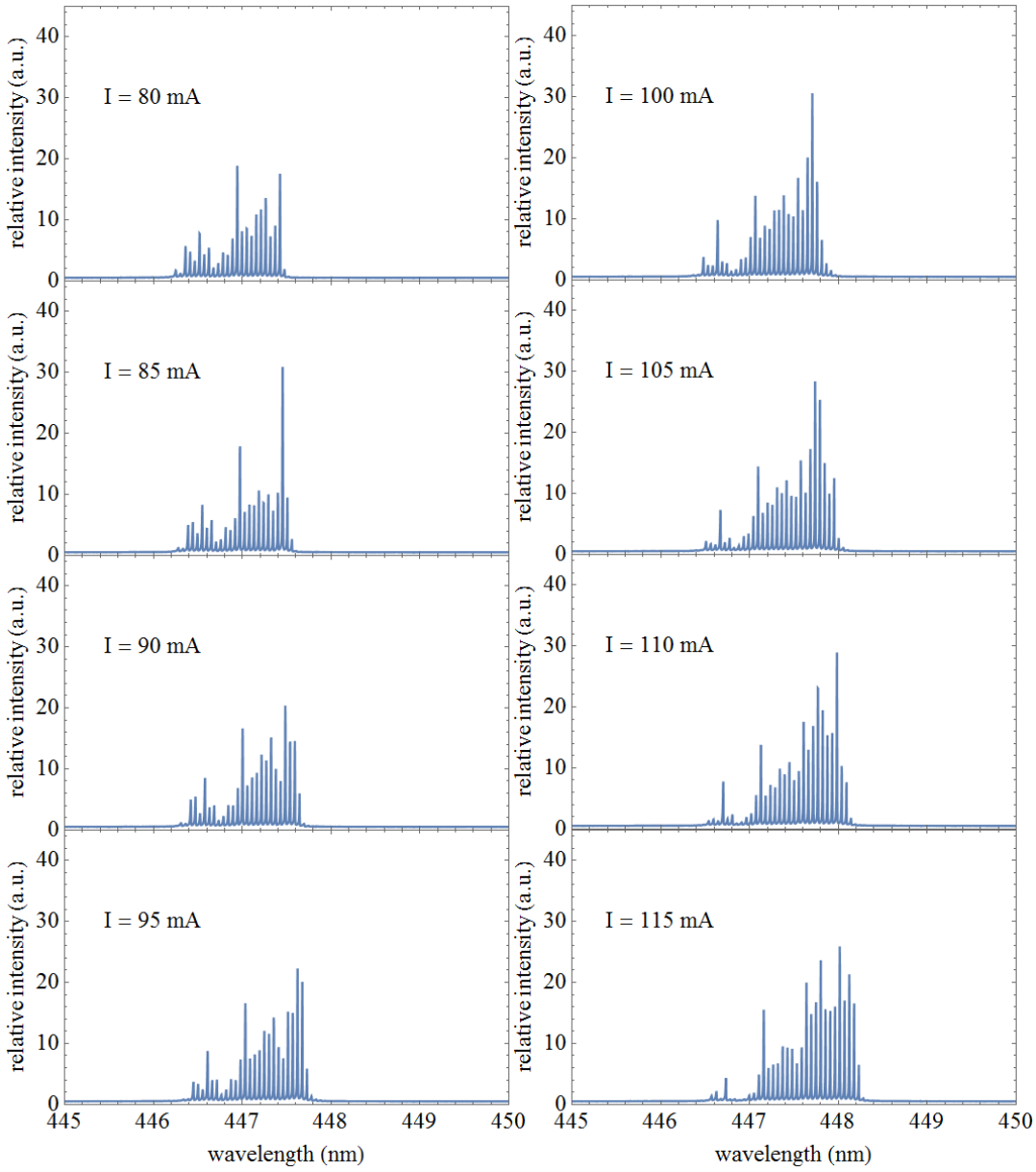

Figure D3: Emission spectra of the GaN blue laser diode at 5 ℃

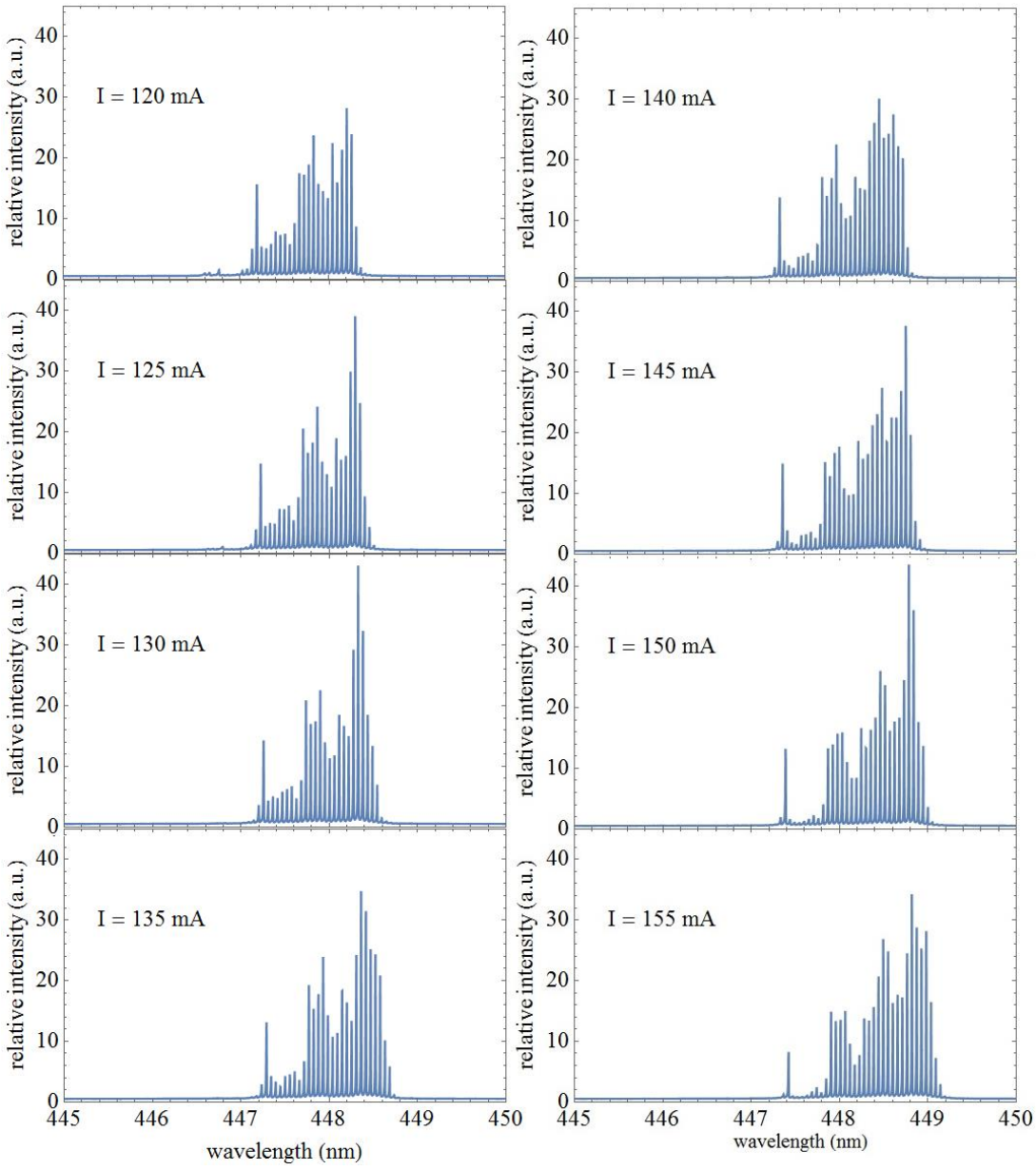

Figure D4: Emission spectra of the GaN blue laser diode at 5 ℃

VITAE

Name:	Taofeek Olawale Adigun
Nationality:	Nigerian
Date of Birth:	8/26/1983
Email:	taofeek.adigun@hotmail.com
Address:	1 Mosalasi Adesan Road, Mowe, Lagos Ibadan Expressway, Ogun State, Nigeria

Academic Background:

1. M. S. in Physics
   King Fahd University of Petroleum and Minerals, Dhahran 31261, Saudi Arabia (2016)
2. B. Tech. in Physics with option in Telecommunications
   Federal University of Technology, Minna, Nigeria (2010)
3. Diploma in Electrical Electronic Engineering
   Osun State Polytechnic, Iree, Nigeria (2005)